Aalto University
School of Electrical Engineering
Doctoral Programme in Electrical Engineering

Suvi Särkijärvi

Atomic layer deposition growth of epitaxial zinc oxide

Licentiate Thesis
Espoo, July 5, 2014

Supervisor: Professor Harri Lipsanen
Advisor: D.Sc. (Tech.) Sami Suihkonen

Aalto University
School of Electrical Engineering
Doctoral Programme in Electrical Engineering

ABSTRACT OF
LICENTIATE
THESIS

Author: Suvi Särkijärvi

Title:
Atomic layer deposition growth of epitaxial zinc oxide

Date: July 5, 2014 **Pages:** viii + 71

Major: Nanotechnology **Code:** S-104

Supervisor: Professor Harri Lipsanen

Advisor: D.Sc. (Tech.) Sami Suihkonen

In this work the basic characteristics of ZnO, atomic layer deposition (ALD) and epitaxial ZnO growth by ALD are presented, followed by the experimental results of the epitaxial growth of ZnO on GaN template by ALD. Diethylzinc (DEZn) and water vapour (H_2O) were used as precursors. The structure and the quality of the grown ZnO layers were studied with scanning electron microscope (SEM), atomic force microscope (AFM), X-ray diffraction (XRD), photoluminescence (PL) measurements and positron annihilation spectroscopy. The ZnO films were confirmed epitaxial, and the film quality was found to improve with increasing deposition temperature in the vicinity of the threshold temperature of two dimensional growth. Contrary to previous reports, high-temperature annealing did not enhance the film properties but rather damaged the film. We conclude that high quality ZnO thin films can be grown by ALD. Interestingly only separate Zn-vacancies were observed in the films, although ZnO thin films typically contain fairly high density of surface pits and vacancy clusters.

Keywords: atomic layer deposition, ALD, epitaxial ZnO

Language: English

Aalto-yliopisto
Perustieteiden korkeakoulu

Aalto-yliopisto
Sähkötekniikan korkeakoulu
Sähkötekniikan tohtoriohjelma

LISENSIAATIN-
TUTKIMUKSEN
TIIVISTELMÄ

Tekijä:	Suvi Särkijärvi		
Työn nimi:	Epitaktisen sinkkioksidin valmistus atomikerrosdepositiomenetelmällä		
Päiväys:	5. heinäkuuta 2014	**Sivumäärä:**	viii + 71
Pääaine:	Nanotekniikka	**Koodi:**	S-104
Valvoja:	Professori Harri Lipsanen		
Ohjaaja:	TkT Sami Suihkonen		

Tässä työssä esitetään sinkkioksidin (ZnO), atomikerrosdeposition (ALD) sekä ALD-menetelmällä valmistetun epitaktisen sinkkioksidin perusominaisuukset. Lisäksi raportoidaan ALD-menetelmällä GaN-alustan päälle valmistettujen ZnO-kalvojen epitaktisuudesta. Lähtöaineina käytettiin dietyylisinkkiä (DEZn) ja vesihöyryä (H_2O). ZnO-kalvojen rakennetta ja laatua tutkittiin elektronisuihkumikroskoopilla (SEM), atomivoimamikroskoopilla (AFM), röntgendiffraktiolla (XRD), fotoluminesenssimittauksilla (PL) ja positroniannihilaatiospektroskopialla. ZnO-kalvojen todettiin olevan rakenteeltaan epitaktisia ja kalvon laadun parantuvan valmistuslämpötilaa nostettassa kaksiulotteisen kasvun kynnyslämpötilan ympäristössä. Vastoin edellisiä raportteja lämpökäsittely ei parantanut kalvojen laatua, vaan tuhosi kalvot. Johtopäätöksenä toteamme, että korkealaatuisia ZnO-ohutkalvoja voidaan valmistaa ALD-menetelmällä. Vastoin odotuksia kalvoissa havaittiin vain yksittäisiä sinkkivakansseja, vaikka ZnO-kalvot sisältävät tyypillisesti suurehkoja määriä kuoppia ja vakanssiryppäitä.

Asiasanat:	atomikerrosdepositio, ALD, epitaktinen ZnO
Kieli:	Englanti

Acknowledgements

This work was carried out at the Department of Micro- and Nanosciences, School of Electrical Engineering, Aalto University, between 2008-2010 and 2013-2014.

I wish to express my gratitude to Professor Harri Lipsanen for supervising my thesis and for giving me the opportunity to work among interesting subjects in the optoelectronics laboratory. I want to thank also M. Sc. Sakari Sintonen, Prof. Filip Tuomisto and M. Sc. Markus Bosund for their contribution for my work. I owe my deepest gratitude to my advisor Dr. Sami Suihkonen for all the invaluable support and consultation with this work.

I want to thank also my husband Jari for all the love and support, and my friends and family for being there for me. The final thanks go to my dear daughters Siiri and Saara, who's tight night's sleep enabled the completion of this work in the end.

This work was supported by the Multidisciplinary Institute of Digitalization and Energy (MIDE) projects Highlight and DEGRADE, the Kaute foundation, the National Graduate School in Material Physics (NGSMP) and the Academy of Finland projects 13138115 and 13251864.

Vantaa, July 5, 2014

Suvi Särkijärvi

Abbreviations and Acronyms

ABE	acceptor-bound exciton
AFM	atomic force microscopy
ALD	atomic layer deposition
ALE	atomic layer epitaxy
CVD	chemical vapor deposition
DAP	donor-acceptor pair
DBE	donor-bound exciton
DEZn	diethylzinc
DMZn	dimethylzinc
DRAM	dynamic random-access memory
DSSC	dye sensitized solar cell
E_c	conduction band energy
E_G	band gap energy
E_v	valence band energy
eV	electron volt, 1.602 176 565 $\cdot 10^{-19}$ J
FRAM	ferroelectric random-access memory
H_2O	water
GaN	gallium nitride
GL	green luminescence
GPC	growth per cycle
IC	integrated circuit
ITO	indium tin oxide
k	crystal momentum
κ	permittivity
LCD	liquid crystal display
LED	light-emitting diode
LO	longitudinal optical phonon
MBE	molecular bean epitaxy
MEMS	microelectromechanical systems
ML	monolayer

MOCVD	metalorganic chemical vapor deposition
MOSFET	metal-oxide-semiconductor field-effect transistor
MOVPE	metalorganic vapor phase epitaxy
O_{Zn}	zinc antisite
PAS	positron annihilaton spectroscopy
PL	photoluminescence
PLD	pulsed laser deposition
RL	red luminescence
RTA	rapid thermal annealing
SEM	scanning electron microscopy
TCO	transparent conducting oxide
TEM	transmission electron microscopy
TES	two-electron satellite transition
TFEL	thin film electroluminescence
TFT	thin film transistor
TTFT	transparent thin-film transistor
UV	ultraviolet
V_O	oxygen vacancy
V_{Zn}	zinc vacancy
XRD	X-ray diffraction
YL	yellow luminescence
Zn_i	zinc interstitial
ZnO	zinc oxide

Contents

Abbreviations and Acronyms **v**

1 Introduction **1**

2 ALD **3**
2.1 Basic characteristics 3
2.2 History 7
2.3 Applications 8

3 ZnO **11**
3.1 Introduction 11
3.2 Chemical properties 12
3.3 Physical properties of crystalline ZnO 13
3.3.1 Lattice structure 13
3.3.2 Electron band structure 16
3.3.3 Defects 20
3.3.4 Doping 22
3.3.5 Optical properties 24
3.4 ZnO thin film growth methods 29
3.4.1 Metalorganic chemical vapor deposition (MOCVD) . . 29
3.4.2 Molecular beam epitaxy (MBE) 29
3.4.3 Pulsed laser deposition (PLD) 30
3.4.4 Sputtering 30
3.4.5 Atomic layer deposition (ALD) 31
3.5 ZnO thin film applications 31

4 Sample preparation **33**
4.1 Template preparation 33
4.2 Cleaning 33
4.3 ZnO growth process by ALD 34
4.4 Annealing 34

5 Thin film characterization **36**
5.1 Scanning electron microscope 36
5.2 Atomic force microscope 37
5.3 X-ray diffraction 38
5.4 Photoluminescence 39
5.5 Positron annihilation spectroscopy 40

6 ALD growth of epitaxial ZnO **42**
6.1 Introduction 42
6.2 Precursors 43
6.3 Requirements for epitaxial growth 43
6.3.1 Temperature 44
6.3.2 Substrates 45
6.3.3 Alternative growth methods 46
6.4 Layer quality 48
6.4.1 Surface morphology 48
6.4.2 Crystalline quality 50
6.4.3 Optical properties 53
6.4.4 Zn vacancies 55
6.4.5 Annealing 56

7 Summary **58**

Bibliography **60**

Chapter 1

Introduction

Zinc oxide (ZnO) is a wide-gap semiconductor with a direct bandgap around 3.4 eV, i.e. in the near-UV region. ZnO holds promises as a material for blue/UV optoelectronics, alternatively to gallium nitride (GaN), and as a cheap, transparent, conducting oxide.[1] The large excitonic binding energy (about 60 meV) of ZnO makes it useful in efficient lasing devices based on stimulated emission due to the recombination of excitons at room temperature.[2] The biggest issue with ZnO future applications is lack of stable and reproducible p-type doping. For example nitrogen doping or codoping could be solutions for p-type ZnO doping problem.[1]

Many methods have been employed to grow epitaxial ZnO films, such as metalorganic chemical vapor deposition (MOCVD)[3], molecular beam epitaxy (MBE)[4], pulsed laser deposition (PLD)[5] and sputtering[6]. However, with atomic layer deposition (ALD) the thickness control, layer uniformity and scalability are superior [7], making it attractive for fabrication of modern semiconducting devices with 3D architecture.[8] Epitaxial ALD growth temperature is also lower than with most of the other methods[9], enabling many low-temperature applications.[8, 10] Strong room-temperature luminescence and high transparency to visible light are properties that enables the epitaxial ZnO applications in optoelectronics and optics.[11] The ALD method is a variant of the chemical vapor deposition (CVD) technique with alternate supply of two precursors.[12]

The number of ZnO ALD publications has increased rapidly since the early 2000's because of the unique features of ALD grown ZnO. However, epitaxial ZnO has gained relatively little interest compared to the large amount of research that has been done on polycrystalline ALD ZnO, mostly because the many potential applications of ZnO thin films do not strictly

require the films to be epitaxial.[11] Polycrystalline ALD ZnO with high-quality electrical properties can be grown in low temperatures, even at room temperature. Doping is a relatively easy procedure in ALD method, and there is currently a lot of research for developing effective ways to produce p-type doping.[13]

The most common precursors for ALD ZnO growth are diethylzinc (DEZn) and water vapour (H_2O). There are several reports on ALD-grown, high-quality epitaxial ZnO on GaN substrate using DEZn and H_2O.[10, 12, 14, 15] The reported threshold temperature for epitaxial growth varies between 250-300 °C. However, there are no reports of growth temperature higher than 300 °C and the surface structure changes with increasing growth temperature have been discussed only briefly.[12]

Annealing enables modifying the film structure after the actual growth process. Annealing causes crystallization and removes defects, and thereby can also improve optical and electrical properties of the film. There are some reports about distinct improvement of ALD ZnO film quality due to annealing in temperature range of 300-1000°C. However, most of the applied templates are sapphire [16, 17] or silicon [18, 19] and in only few cases the ALD growth temperature is higher than 200°C [20, 21]. There are no reports about annealing clearly epitaxial ALD ZnO samples on GaN template.

In this work the chapters 2 and 3 present the basic characteristics of ZnO and ALD method and their applications. Chapters 4 and 5 describe the experimental part of this work: sample preparation and the characterization methods. In chapter 6 the theoretical background of epitaxial growth of ZnO by ALD is discussed, followed by the experimental results of the epitaxial growth of high quality ZnO films on GaN templates by ALD method. The film quality is comprehensively studied and the effect of ALD process temperature on the film properties is discussed. In addition to previous reports, the ZnO layer structure is thoroughly characterized in the vicinity of the threshold temperature of two dimensional growth, applying also SEM and positron annihilation spectroscopy. The samples were annealed after the characterization to study the annealing effects on the epitaxial ZnO films.

Chapter 2

ALD

This chapter presents the basic characteristics of atomic layer deposition (ALD) method, its history and some ALD applications.

2.1 Basic characteristics

ALD can be defined as a thin film deposition technique that is based on the sequential use of self-terminating gas-solid reactions. The ALD method is a variant of the chemical vapor deposition (CVD) technique (see Section 3.4.1) with alternate supply of two precursors.[12] The ALD growth process consists of repeating the following characteristic four steps illustrated in Figure 2.1: 1) self-terminating reaction of the first reactant A, 2) purge with an inert gas (typically nitrogen or argon) or evacuation to remove the nonreacted reactants and the gaseous reaction by-products, 3) self-terminating reaction of the second reactant B and 4) another purge or evacuation. Reactants are often called as precursors. Steps 1-4 constitute a reaction cycle. Steps 1 and 3 are sometimes referred to as half reactions of an ALD reaction cycle. Each reaction cycle adds a given amount of material to the surface, referred to as the growth per cycle GPC.[22] Only in an ideal case a monolayer (ML) per cycle is formed. In practice, due to steric hindrances, one reaction cycle usually produces only a distinct fraction of a monolayer, e.g. up to 1/2 ML.[23] To grow a certain thickness of layer, reaction cycles are repeated until the desired amount of material has been deposited. Before starting the ALD process, the surface is stabilized for example by cleaning or by a heat treatment. Due to the self-terminating reactions ALD is a surface-controlled process, where process parameters other than the reactants, substrate, and temperature have little or no influence. Because of the surface control, ALD-grown films are extremely conformal and uniform in thickness.[22]

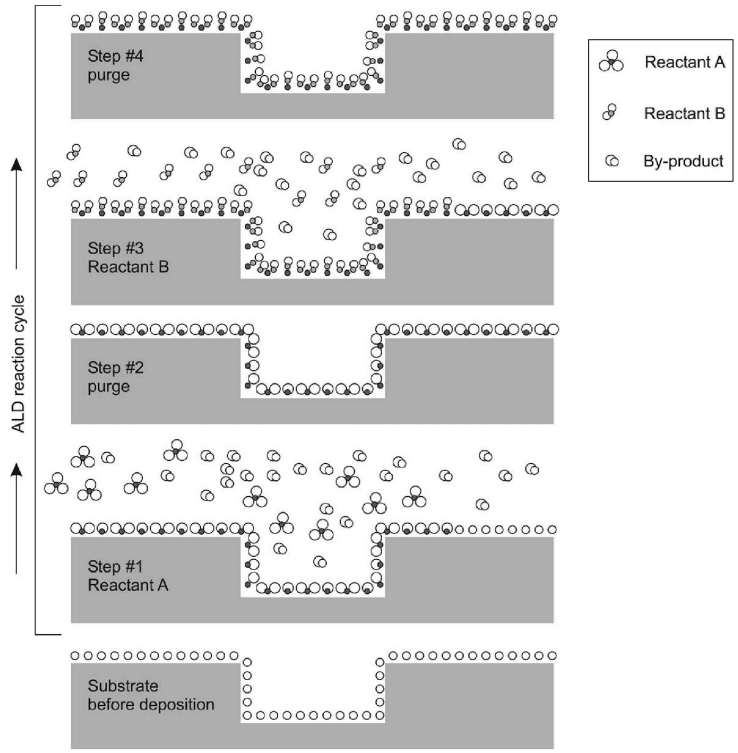

Figure 2.1: ALD reaction cycle consisting of four steps; gas-solid reaction of the first precursor (reactant A), purge, gas-solid reaction of the second precursor (reactant B) and another purge.[22]

The ALD growth window (Figure 2.2) indicates the temperature range where thin film growth proceeds by surface control, i.e. the growth rate is stable. Outside the ALD growth window the growth is limited by precursor condensation, decomposition and desorption or by insufficient reactivity (activation energy not achieved). The growth rate is usually lower outside the ALD the growth window. Typically the lowest growth temperatures result in amorphous film structure, the temperatures around the growth window produce polycrystalline film and epitaxial film is achieved with considerably higher temperatures than the ALD growth window. The surface control of ALD is supported by the fact that the precursor pulse length (dose) has no effect on the growth rate provided that the surface is saturated, i.e. all available surface sites are occupied by adsorbed precursor molecules. However, some organometallic precursors for oxide films do not exhibit a distinct ALD window and thus the deposition rate in these processes is dependent on the temperature, but nevertheless they can still be used for self-limiting ALD

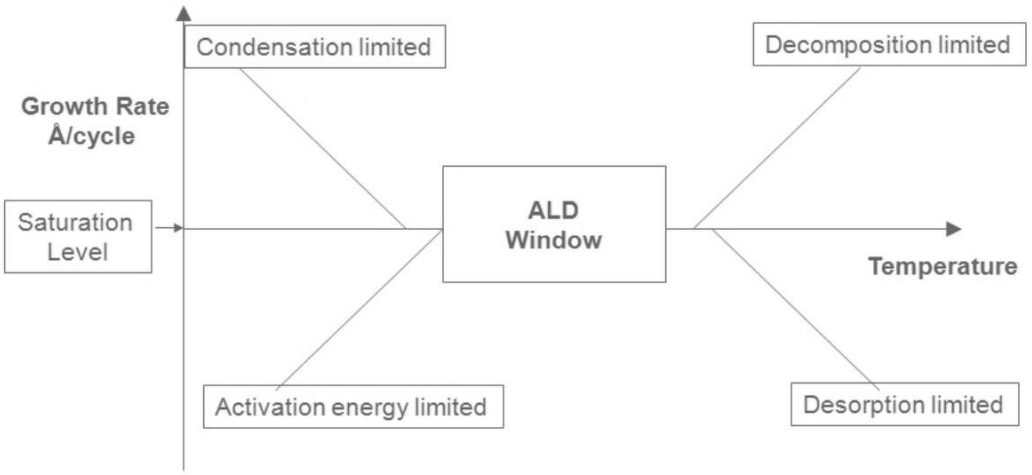

Figure 2.2: ALD growth window limited by precursor condensation, insufficient reactivity, precursor decomposition and precursor desorption. If the deposition rate is dependent on the number of available reactive sites, actual ALD window cannot be observed.[24]

processes. This has been explained by their high reactivity towards reactive surface sites, typically OH groups, whose amount is dependent on the deposition temperature.[23]

Precursor chemistry plays a key role in ALD. The precursors must be volatile and thermally stable at the deposition temperature.[25] In addition to gaseous precursors, also liquid and solid precursors are possible to use, but they have to be vaporizable at temperatures lower than the ALD reaction temperature to enable transportation through the gas phase. In practice it requires special source designs for the ALD reactor.[13] Precursors must chemisorb on the surface or react rapidly with the surface groups and react aggressively with each other. In that way it is possible to reach the saturation stage in a short time (less than 1 s) and thereby ensure a reasonable deposition rate; low deposition rate is a typical feature of ALD processing.[25] The precursors are not allowed to etch the substrate or the growing film or dissolve in the film.[13, 23] Most ALD processes are based on binary reaction sequences where two surface reactions occur and deposit a binary compound film.[7] Processing of ternary and more complicated compounds requires the constituent precursors to volatilize and then react at a common temperature (ALD growth window) because during the growth process the reactor temperature cannot be changed. By suitable selection of precursor chemistry the

processing temperatures of ALD can be relatively low. Also doping of the films during the growth process is relatively simple.[23]

The self-limiting aspect of ALD leads to excellent step coverage and conformal deposition on high aspect ratio structures. Some surface areas will react before other surface areas because of different precursor gas fluxes. However, the precursors will adsorb and subsequently desorb from the surface areas where the reaction has reached completion. The precursors will then proceed to react with other unreacted surface areas and produce a very conformal and pinhole-free deposition. ALD processing is also extendible to very large substrates and to parallel processing of multiple substrates. Because the ALD precursors are gas phase molecules, they fill all space independent of substrate geometry. ALD is only limited by the size of the reaction chamber. Because the surface reactions are performed sequentially, the two gas phase reactants are not in contact in the gas phase. This separation of the two reactions limits possible gas phase reactions that can form particles that could deposit on the surface to produce granular films.[7]

The substrate quality affects on the structure of the growing film, because the grain boundaries and other structural defects of the substrate are copied to the new layers. This occurs by some extent also with polycrystalline and amorphous films, but is fundamental in the case of epitaxial films where the substrate has to be lattice-matched to the growing film to ensure the layer quality. Even though the substrate can be porous or of any kind of shape, in some cases the ALD growth is not possible if the substrate surface is completely inert; there are no reaction sites for the ALD growth.[26]

The conventional ALD method is called thermal ALD, where the growth temperature is sufficient for maintaining the chemical reactions. Most of the thermal ALD grown materials are binary compounds based on binary reactant CVD processes. The wide variety of thermal ALD grown thin films includes various oxides (e.g. Al_2O_3, TiO_2, SnO_2, ZnO, HfO_2), metal nitrides (e.g. TiN, TaN, W_2N), metal sulfides (e.g. ZnS, CdS) and phosphides (e.g. GaP, InP). However, there is also a need for single-element ALD materials, such as metals and semiconductors, that can be deposited using a binary reaction sequence. The single-element films of metals and semiconductors are usually very difficult to deposit using thermal ALD processes. These single elements can be deposited using plasma or radical-enhanced ALD. The radicals or other energetic species in the plasma help to induce reactions that are not possible using only thermal energy. For example single-element semiconductors Si and Ge can be deposited using hydrogen radical-enhanced

ALD. In addition to single-element materials, plasma-enhanced ALD can deposit compound materials. One important advantage is that plasma-enhanced ALD can deposit films at much lower temperatures than thermal ALD.[7] On the contrary, thermal ALD processes fulfill best the requirement of self-terminating reactions on complex three-dimensional (3D)substrates. In "energy-enhanced" processes, typically utilizing energetic but unstable reactants such as ozone or plasma, problems with conformality may arise through reactant decomposition at least on 3D substrates.[22]

2.2 History

There are two different versions of the origin of the ALD method. According to the more commonly acknowledged origin ALD was introduced 1974 in Finland by Tuomo Suntola and co-workers under the name of atomic layer epitaxy (ALE). The first materials deposited by ALD were ZnS, SnO_2 and GaP with elemental precursors.[27]. The research originated by Suntola and co-workers has led to commercial applications of ALD for making thin-film electroluminescent (TFEL) displays already in the 1980s. The less commonly acknowledged origin of ALD is the work made in the Soviet Union in the 1960s by the group of Professor Aleskovskii. Their first deposition materials were TiO_2 and GeO_2 by the method called molecular layering (ML).[22]

In the 1980's ALD was developed mostly in Finland and neighboring Baltic countries. Deposition of a range of different materials was demonstrated at that time, including II-VI semiconductors (e.g. CdTe, CdS) and III-V (e.g. GaAs, GaN), with possible applications in e.g. photovoltaics.[28] The name "atomic layer deposition" dates back to the early 1990s. The reason for the name change was that the films grown by ALD are commonly polycrystalline or even amorphous, while the term "epitaxial" implies a crystalline ordering with the underlying substrate.[22]

A real boom in interest came in early 2000's with the development of deposition methods of thin films of high-κ dielectrics. This research was motivated by a high leakage current in field-effect transistors with SiO_2-based gate dielectrics. In 2007 Intel introduced a new generation of integrated circuits (ICs) with thin films of HfO_2 used as gate isolating layers. In these and following ICs the films of HfO_2 are deposited by ALD.[28] The reason is the unique properties of the ALD films; ALD is considered a deposition method with great potential for producing very thin, conformal films with control of the thickness and composition of the films possible at the atomic

level. A major driving force for the recent interest is the prospective seen for ALD in scaling down microelectronic devices.[7]

2.3 Applications

The ALD method has a wide range of possible applications, such as microelectronics, nanotechnology, optoelectronics and energy applications. Most ALD processes are based on binary reaction resulting in a binary compound film[7] but the number of ternary compounds studied in ALD is increasing. The ternary compounds studied are mainly multi-component oxides. Interest in them arises from their high dielectric constant, ferroelectric properties and magnetic properties.[13]

The first ALD application (and also the original reason for developing the ALD method) was flat panel display based on thin film electroluminescence (TFEL). The industrial production started in 1983. The TFEL flat panel display consist of a stack of thin film layers on a glass substrate through which the display is viewed. In the simplest case (a monochromatic yellow-emitting display) the TFEL structure contains a semiconducting light-emitting core (Mn-doped ZnS) surrounded by dielectric layers (Al-Ti-oxide). In addition, a transparent front electrode (In-Sn-oxide, ITO) and a back electrode (Al) are needed together with passivation and ion barrier layers. All layers, except for the Al back electrode, can be deposited and doped by ALD.[29]

Microelectronics has been the most important application area motivating the ALD research; high-κ oxides for both transistors and DRAM capacitors have formed the largest focus area. New processes have been developed for Group IV metal oxides (ZrO_2, HfO_2) but doping of the oxide films, making of nanolaminates and ternary compounds have been important part of the research aiming for increase of the κ-value and more stable films.[13] The need for high-κ oxides arises from overly high tunneling current through the commonly used SiO_2 gate dielectric in metal-oxide-semiconductor field-effect transistors (MOSFETs) when it is downscaled to a thickness of 1.0 nm and below.[30] A thicker gate dielectric can be employed for the required capacitance density by applying high-κ oxide, such as Al_2O_3, ZrO_2 and HfO_2 and also multilayer structures (ZrO_2 - Al_2O_3 - ZrO_2)[13], thus the tunneling current can be reduced through the structure.[30] The further step to higher-κ materials is the adoption of ternary oxides. Aluminates, especially $LaAlO_3$, have been of interest, because it makes a stable structure on Si, contrary to pure La_2O_3.[13]

The development of dynamic random access memory (DRAM) capacitor dielectrics has been similar to the gate dielectrics: SiO_2 has been widely used in the industry thus far, but it is likely to be phased out in the near future as the scale of devices are decreased. The requirements for the downscaled DRAM capacitors are good conformality and low permittivity, thus the candidate materials are different from those explored for MOSFET gate dielectrics.[31] The most promising candidates have been ternary compounds $BaTiO_3$ and $SrTiO_3$. The limited Sr precursor chemistry has slowed down the industrial use of ALD grown $SrTiO_3$.[13]

Microelectronics has also motivated the development of ALD processes for metal and conducting metal oxide films to be used as electrodes. Noble metal and noble metal oxide films and especially the interfacial behavior between dielectrics and metal electrodes have received a lot of attention. Phase-change materials for non-volatile electronic memories, such as ferroelectric random access memory (FRAM), present a new area for ALD. For that application, new chemistry and processes to deposit germanium and antimony tellurides have been developed. Ferroelectric materials are usually ternary or quaternary oxides, such as $BaTiO_3$, $SrTiO_3$ and $PbZrO_3$.[13]

Ferromagnetic materials are used in spintronics to generate spin-polarized current at and above room temperature.[32] Metal oxide semiconductors exhibiting room-temperature ferromagnetism (RTFM) have been investigated extensively and of particular interest are diluted magnetic semiconductors (DMSs), which are nonmagnetic semiconductors such as TiO_2, ZnO, AlN, or GaN modified by the addition of small atomic percentages of open-shell transition metal (TM) dopants, such as Cr, Mn, Fe and Co.[33] ALD is promising growth method for these kind of applications.

Transition-metal nitrides, such as TiN and TaN, are being used both as metal barriers and as gate metals.[30] Metal barriers are employd in Cu-based chips to avoid diffusion of Cu into the surrounding materials, such as insulators and the silicon substrate. Also Cu interconnections are surrounded with a layer of metal barriers in order to prevent Cu contamination by elements diffusing from the insulators.[34]

MEMS and different nanotechnology applications are naturally suited for ALD. It is very effective method for high-aspect ratio coating of any nanostructured devices and materials, such as nanopores, nanowires and -tubes, nanopatterning and nanolaminates.[29] No new processes have been developed but existing well-working processes such as those for Al_2O_3, TiO_2 and ZnO have been applied. Protective (barrier) layers and optoelectronics form other important and increasing application areas. They also mostly rely on

existing processes but for optics new chemistry has been studied for metal fluoride films.[13] The surface passivation of silicon solar cells with ALD grown Al_2O_3 to ensure minimal surface recombination losses has shown excellent results.[35] Transparent conducting oxides (TCO) are important optoelectronics application for ALD. TCO films are needed for example in thin-film solar cells and light-emitting diodes (LEDs) as current spreading layer. ALD deposited ZnO is a strong candidate for these applications.[36] In the case of protective films, the substrate to be covered is often polymer material, setting limitations for the process temperature.[13] Silver jewelry can be coated with ALD for preventing tarnishing. Tarnishing is mainly caused by airborne sulfur, which reacts with the surface of silver and produces black silver sulfide (Ag_2S).The anti-tarnish coating is a two-component thin film consisting of Al_2O_3 and TiO_2 layers. While the bottom layer acts as a bonding layer with good adherence to the silver, the top layer acts as a barrier layer through which liquids and other aggressive chemicals cannot penetrate.[37]

Another growing area for ALD technology is energy applications, such as energy conversion (photovoltaics, fuel cells, photoelectrochemical cells) and energy storage (lithium batteries, ultracapacitors). Nanostructured materials are likely to have an important role in utilizing renewable energy sources. ALD is a useful technology for synthesizing nanomaterials by functionalizing porous scaffolds to impart the desired chemical, physical, or electronic properties. For instance, the wide scale applications of lithium batteries require substantial improvements in their lifetime.[38] New ALD processes have been developed for lithium containing films, such as ternary or quaternary films.[13] Ultrathin ALD Al_2O_3 films applied to porous $LiCoO_3$ cathode powders improves dramatically the charge/discharge cyclability of lithium batteries. In the area of photovoltaics, dye sensitized solar cells (DSSC) offer the potential for low-cost solar power using widely available materials, but currently the relatively low conversion efficiencies of DSSC have limited their adoption. ALD has yielded promising results with ultrathin transparent conducting films, dye adhesion layers and barrier films into the DSSC structure that could be combined with improved electrolytes and sensitizers to make a highly efficient DSSC suitable for low cost mass production.[38]

Chapter 3

ZnO

This chapter presents the basic chemical and physical properties of ZnO and the common growth methods and applications of ZnO thin films.

3.1 Introduction

Zinc oxide is a II-VI compound semiconductor. It has a direct wide bandgap around 3.4 eV, i.e in the near-UV region and it crystallizes preferentially in the hexagonal wurtzite-type structure. ZnO appears as a white powder and in nature it occurs as mineral zincite. It is widely used as an additive in several materials and products (such as concrete and rubber) [1], but also increasingly in optoelectronics because of its favorable properties: good transparency, high electron mobility, wide bandgap and strong room temperature luminescence. Those properties are already used i.e in transparent electrodes in liquid crystal displays (LCDs), thin-film transistors (TFTs) and light-emitting diodes (LEDs). ZnO is a promising material to replace gallium nitride (GaN) in optoelectonic applications; they share the lattice structure, and the lattice parameters and band gap are close to each other. The crystal growth technology for high-quality ZnO bulk single crystals is much simpler and cheaper compared to GaN. ZnO has also a large exciton binding energy (60 meV) compared to other wide-band-gap semiconductors and it makes ZnO useful in efficient lasing devices based on stimulated emission due to the recombination of excitons also at room temperature. However, the biggest issue with the future applications of ZnO is to achieve high, stable and reproducible p-type doping.[2]

Research on ZnO started gradually in the 1930s. There was an intensive research peak around the end of the seventies and the beginning of the

eighties. The emphasis of ZnO research at that time was essentially on bulk samples covering topics such as growth, doping, transport, band structure, excitons, bulk and surface polaritons, luminescence, high excitation or many-particle effects and lasing. Later the interest faded because it was not possible to dope ZnO in both an n- and p-type manner, which is an indispensable prerequisite for applications of ZnO in optoelectronics. Another reason was that the interest shifted to structures of reduced dimensionality, like quantum wells.[39]

The present high season in ZnO research started in the mid 1990s and the interest has been focused on growing epitaxial layers, quantum wells, nanorods and related objects or quantum dots. The most interesting topics for the current ZnO research are to obtain suitable material for blue/UV optoelectronics including light emitting diodes or even laser diodes in addition to the GaN-based structures, radiation-hard material for electronic devices in a corresponding environment, transparent material for electronic circuits that is usable at elevated temperatures, diluted- or ferromagnetic material that is suitable for semiconductor spintronics and transparent, highly conducting oxide (TCO) to replace expensive indium tin oxide (ITO). A stable, high and reproducible p-type doping is obligatory for several of the above-mentioned applications. Though progress has been made in this crucial field, this aspect still represents a major problem. [1]

3.2 Chemical properties

Zinc oxide is an inorganic compound with the formula ZnO. It occurs as a water-soluble, odorless white powder. In nature it occurs as mineral zincite but most of the industrial used zinc oxide is produced synthetically. Pure ZnO is colourless and clear due to its large bandgap. The mineral zincite contains typically manganese and other impurities, resulting in yellow or red color.[1, 39] Because of its thermochromic nature, crystalline zinc oxide changes its colour from white to yellow when heated and reverts to white on cooling. The color change is originated from a small loss of oxygen at high temperatures, forming the non-stoichiometric $Zn_{1+x}O$ where x=0.00007 at 800°C.[40]

At around 1975°C ZnO decomposes into zinc vapor and oxygen. Heating with carbon converts ZnO into zinc vapor at a much lower temperature; around 950°C.[41]

3.3 Physical properties of crystalline ZnO

ZnO is a semiconductor compound of the group II element zinc and the group VI element oxygen. Zinc has the electron configuration $1s^2 2s^2 2p^6 3s^2 3p^6 3d^{10} 4s^2$ and the oxygen configuration is $1s^2 2s^2 2p^4$. The ZnO binding in its crystal lattice involves sp^3 hybridization of the electron states, leading to four equivalent orbitals in tetrahedral geometry.[42] In the resulting semiconductor crystal the highest valence band is formed of the occupied 2p orbitals of O^{2-} or the binding sp^3 orbitals in the outer shells of ZnO and the lowest conduction band of the empty 4s states of Zn^{2+} or the antibinding sp^3 hybrid states.[1] The number three in sp^3 hybridisation refers to that the zinc-oxygen bond consists of 25 % s-character and 75 % p-character (1 : 3).

3.3.1 Lattice structure

Most of the II-VI binary compound semiconductors exist either in cubic zincblende or hexagonal wurtzite or both, such as ZnS, which gave the name both to the structures.[39] In both forms one anion is surrounded tetrahedrally by four cations and vice versa. This tetrahedral coordination is typical of sp^3 covalent bonding, but these materials also have a substantial ionic character. However, the ionicity of ZnO resides at the borderline between covalent and ionic semiconductor. Zinc oxide crystallizes with great preference in the hexagonal wurtzite-type structure, but also the cubic zincblende and rocksalt forms are possible.[1] The crystal structures of them are presented in Figure 3.1.

At ambient conditions the hexagonal wurtzite ZnO (Fig. 3.1(c)) is thermodynamically stable phase. The cubic zincblende (Fig. 3.1(b)) ZnO can be stabilized to some extent by growing ZnO epitaxially on suitable substrates with cubic zincblende lattice structure, such as ZnS[44] or GaAs/ZnS[45]. In the case of highly mismatched substrates, there is usually a certain amount of zincblende phase of ZnO separated by crystallographic defects from the wurtzite phase.[2] The zincblende structure ZnO can not be achieved by applying pressure to other forms.

The rocksalt structure (Fig. 3.1(a)) can be obtained by applying relatively high pressure to wurtzite ZnO (about 100 kbar). The reduction of the lattice dimensions causes the interionic Coulomb interaction to favor the ionicity of

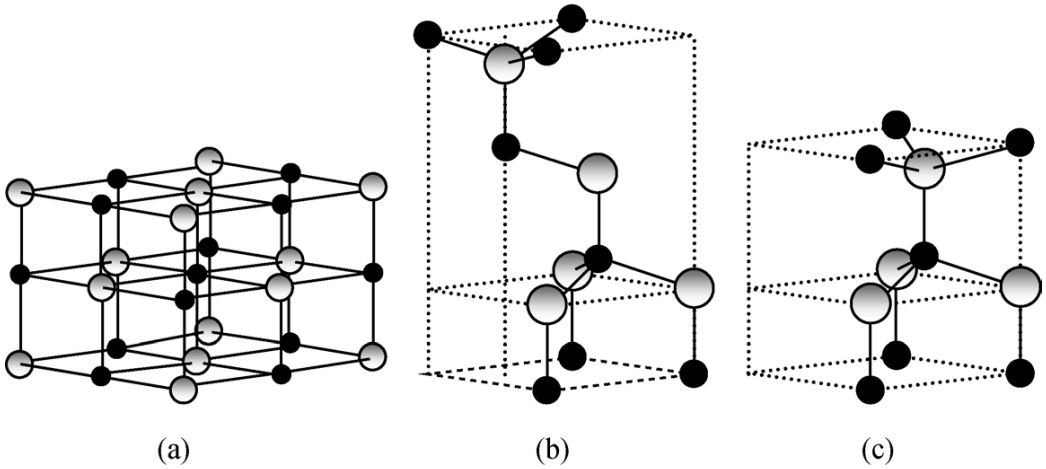

Figure 3.1: Three possible lattice structures of ZnO: (a) Cubic rocksalt (b) Cubic zincblende (c) Hexagonal wurtzite. The grey spheres denote Zn atoms and black spheres O atoms.[43]

more over the covalent nature. The rocksalt structure cannot be stabilized by epitaxial growth.[2] It is also theoretically calculated that the rocksalt structure can transform to CsCl (cesium chloride) structure at applied transition pressure of about 2.6 Mbar. CsCl structure is a primitive cubic lattice with a two-atom basis, where both atoms have eightfold coordination.[46]

The wurtzite structure in Figure 3.2 is composed of two interpenetrating hexagonal-close-packed (hcp) sublattices, each of which consists of one type of atom displaced with respect to each other along the threefold c-axis by the amount of u=3/8=0.375 (in an ideal wurtzite structure) in fractional coordinates. The u parameter is defined as the length of the bond parallel to the c-axis in units of c. In the plane perpendicular to the c-axis, the primitive translation vectors a and b have equal length and include an angle of 120°. Each sublattice includes four atoms per unit cell and every atom of one kind (group II atom) is surrounded by four atoms of the other kind (group VI) or vice versa, which are coordinated at the edges of a tetrahedron. The wurtzite primitive unit cell contains two pairs of ions (two ZnO units). In a real ZnO crystal the wurtzite structure deviates from the ideal arrangement by changing the c/a ratio or the u value.[2, 42]

The empirically proven lattice constants for wurtzite type ZnO at room temperature are a=b=3.249 Å and c=5.206 Å. Their ratio c/a=1.60 is close

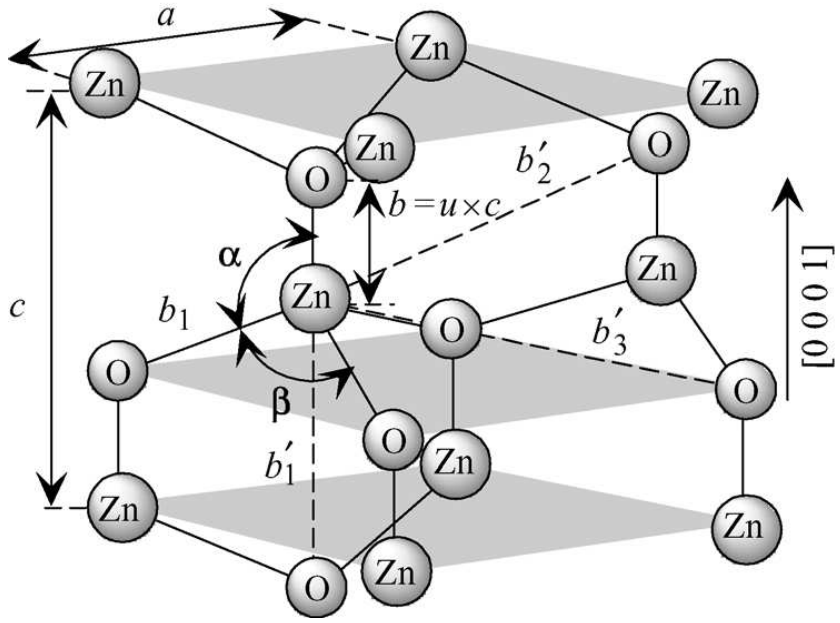

Figure 3.2: Lattice structure of wurtzite type ZnO. Lattice constant a is in the basal plane and c in the basal direction. The u parameter is defined as the bond length or the nearest-neighbor distance b divided by c. α and β (both 109.47° in ideal crystal) are the bond angles.[43]

to the ideal value for hexagonal cell c/a=1.633.[47]

The zincblende structure (Fig. 3.1(b)) may be regarded as an arrangement of two interpenetrating face-centered cubic sub-lattices, displaces by 1/4 of the body diagonal axis. The bonding orbitals are directed along the four body diagonal axes. The cube unit cell is not the smallest periodic unit of a zincblende crystal, so it is not a primitive unit cell. The primitive unit cell of zincblende is an oblique parallelepiped and in contrast to wurtzite, zincblende unit cell contains only one pair of ions (only one ZnO unit).[42]

The bonding in ZnO is largely ionic (Zn^{2+}-O^{2-}) with a considerable degree of polarity. The corresponding ionic bond radius is 0.74 Å for Zn^{2+} and 1.40 Å for O^{2-}, i.e. their ratio is roughly 1:2. This property is responsible for the preferential formation of wurtzite rather than zincblende structure.[42] Hexagonal and zincblende structures do not possess inversion symmetry, i.e reflection of a crystal relative to any given point does not transform it into itself. Thus the crystal exhibits crystallographic polarity, which indicates the

directions of the bonds. This and the (partially) ionic binding of ZnO are the origin of the piezoelectricity of the hexagonal and zincblende ZnO.[1]

3.3.2 Electron band structure

ZnO is a wide-gap semiconductor with a direct band gap of ∼3.4 eV at room temperature. The band gap represents the minimum energy difference E_g between the upmost valence band and the lowest conduction band. They are each characterized by a crystal momentum, k-vector. If the both band extrema are at the same point in the Brillouin zone, namely at k=0, the energy gap is called direct.[1] Thus an electron from the conduction band can directly recombine with a hole in the valence band, emitting a photon (Figure 3.4(a)). The k-axis is split into regions by the effect of the periodic lattice potential on the electron states. These regions are called Brillouin zones and the region containing the band gap is the first Brillouin zone ($|k| < \pi/a$), as in Figure 3.3.[48]

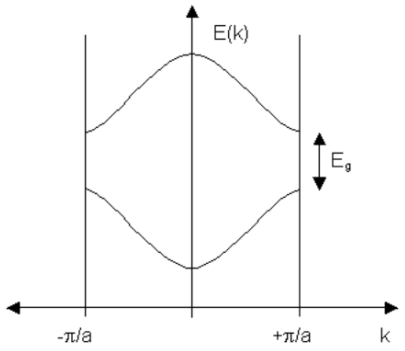

Figure 3.3: First Brillouin zone. E_g denotes to the band gap.[49]

In the case of indirect band gap the maximum energy of the valence band occurs at a different value of momentum (in the k-axis) than the minimum of the conduction band energy. An electron in the conduction band has to gain (or loose) momentum to move to the valence band and to recombine with a hole. To change its momentum an electron has to for example interact with a lattice vibration called a phonon or go through some defect state within the band gap (Figure 3.4(b)).[51]

The energy bands of a semiconductor are result of the crystal potential that originates from the equilibrium arrangement of atoms in the lattice. The outermost valence electrons of semiconductors are in s- or p-type orbitals. If

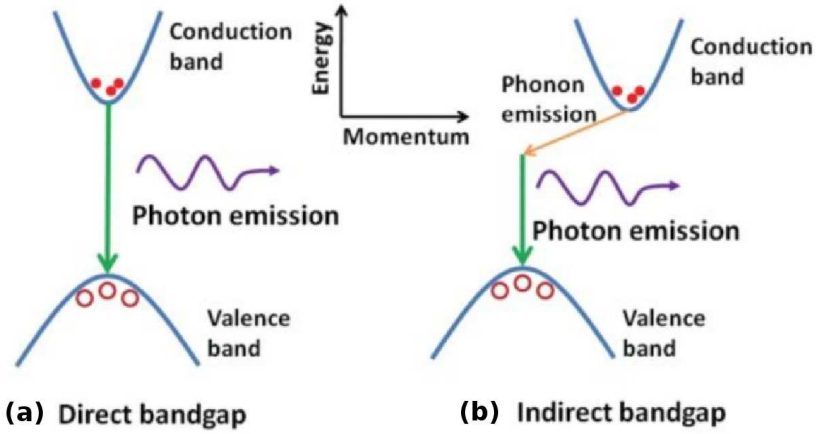

Figure 3.4: (a) Direct and (b) indirect band gap. In the case of the direct band gap, an electron from the conduction band can directly recombine with a hole in the valence band, emitting a photon. With indirect band gap an electron needs for example a phonon interaction to change its momentum.[50]

the edge of the conduction band is made up of s-type states, the semiconductor has a direct bandgap. If the lowest conduction band edge is made up of p-type states, the bandgap is indirect.[52] For ZnO, the lowest conduction band is formed from the empty 4s states of Zn^{2+} or the antibinding sp^3 hybrid states. The valence band originates from the occupied 2p orbitals of O^{2-} or the binding sp^3 orbitals.[1]

Hexagonal wurtzite ZnO belongs to the crystallographic point group C_{6v} (in Schoenflies notation); it has 6-fold rotation axis and 6 mirror planes containing the axis of rotation.[54] In the hexagonal wurtzite-type lattice the high-symmetry points of Brillouin zone are denoted by capital (Latin) letters and directions of high symmetry by capital Greek letters, as in Figure 3.5. The center of the Brillouin zone, where k=0, is denoted by Γ.[53]
Spin-orbit coupling causes the splitting of energy bands near the Γ-point, and the valence bands are also effected by crystal field splitting. The spin-orbit coupling originates from electromagnetic interaction between the electron spin and the orbital angular momentum. The crystal field splitting is caused by the effect of the electrical field of neighboring ions on the energies of the valence band orbitals of an ion in the crystal.[55] The valence bands are split without spin under the influence of the hexagonal crystal field into two states and inclusion of spin gives a further splitting due to spin-orbit coupling into three sub-valence bands. These valence bands are labelled in all

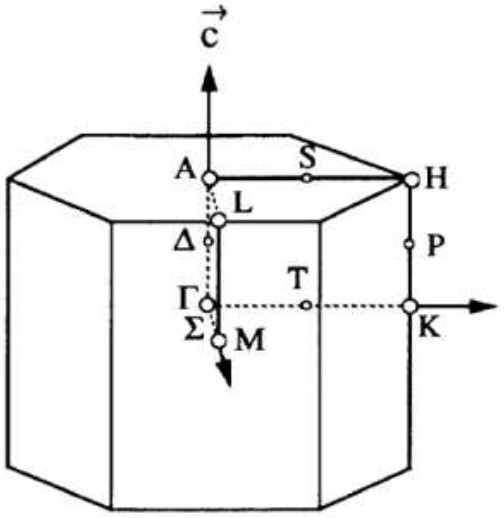

Figure 3.5: First Brillouin zone of the hexagonal wurtzite-type structure (C_{6v}). The points of high symmetry are labelled by capital (Latin) letters and directions of high symmetry by capital Greek letters.[53]

wurtzite-type semiconductors (such as ZnS, CdS and GaN) from higher to lower energies as A, B and C bands, as displayed in Figure 3.7.[1, 56]

The ZnO electron band structures are different for the different lattice structures. In Figure 3.8 there are band structures for (a) hexagonal wurtzite ZnO, (b) cubic rocksalt and (c) cubic zincblende. The hexagonal structure is the stable form at ambient conditions and it will transform to rocksalt form under applied transition pressure of about 100 kbar.[2] When a phase is converted to another by applying pressure, there are changes in the nearest-neighbor bond lengths and in lattice symmetry. These changes effect on the band overlaps, bandwidths, the *p-d* hybridization and band repulsion. As the neighboring atoms approach each other with compression of the solid, basis functions overlap more strongly, producing increased dispersion of the electron bands in the k-space and consequently increased bandwidths along the energy axis.[2]

Advantages associated with a large band gap include higher breakdown voltages, ability to sustain large electric fields, lower electronic noise generation and high-temperature and high-power operation. The bandgap of ZnO can further be tuned to about 3-4 eV by alloying it with magnesium oxide

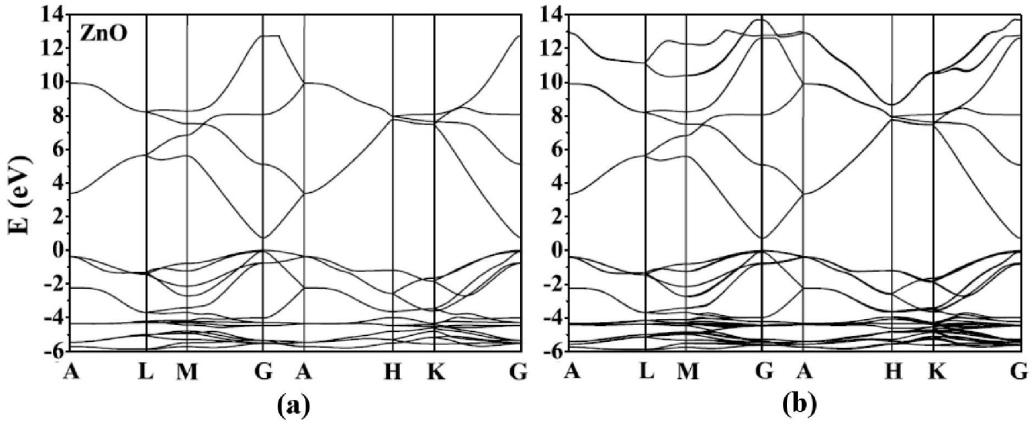

Figure 3.6: Band gap structure of wurtzite ZnO (a) without and (b) with spin-orbit coupling. The x-axis represent the lines of symmetry in the Brillouin zone of hexagonal lattice.[56]

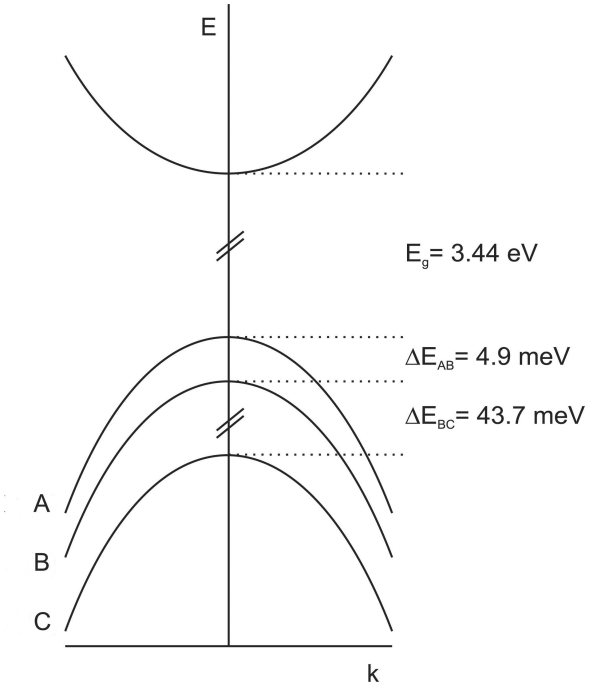

Figure 3.7: Crystal-field and spin-orbit splitting of the valence band of wurtzite ZnO into 3 subbands A, B and C at 4.2 K.[57]

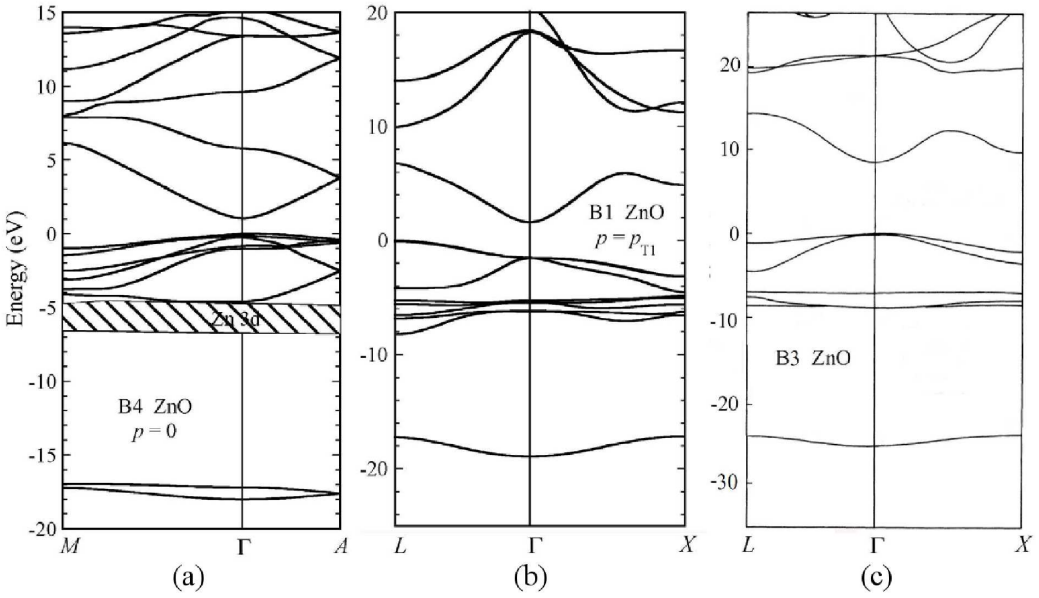

Figure 3.8: Band structure for (a) hexagonal wurtzite at $p = 0$ [43] (b) cubic rocksalt at $p = p_{T1}$ [43] (c) cubic zincblende ZnO [58].

or cadmium oxide.[2]

3.3.3 Defects

Defects are forms of deviations from unexcited, infinite, ideal crystal structure. Semiconductor defects can be divided into volume, surface, line and point defects. Point defects are of atomic size and include vacancies, interstitials, substitutionals (impurity atoms) and antisites (where two atoms of different type have exchanged their positions in a compound lattice), as illustrated in Figure 3.9. Only point defects have low enough formation energies to be formed by thermal activation. At any temperature there are equilibrium concentrations of native point defects. All the larger defects occur only as the result of accidents of growth and processing.[59]
Point defects are considered to be the most important group of defects in semiconductors, because impurity doping determines device properties and the interactions of the doping atoms with other point defects can alter their effects.[59] Point defects affect the electrical and optical properties of ZnO as well as in any semiconductor.[2]
Point defects can act as acceptors and donors. They are called shallow or deep, depending on their ionization energy. Shallow acceptors and donors

require little energy to ionize; typically around the thermal energy or less. Deep acceptors and donors require energies larger than the thermal energy to ionize.[51] There is more detailed information about deep and shallow acceptors in the Section 3.3.4.

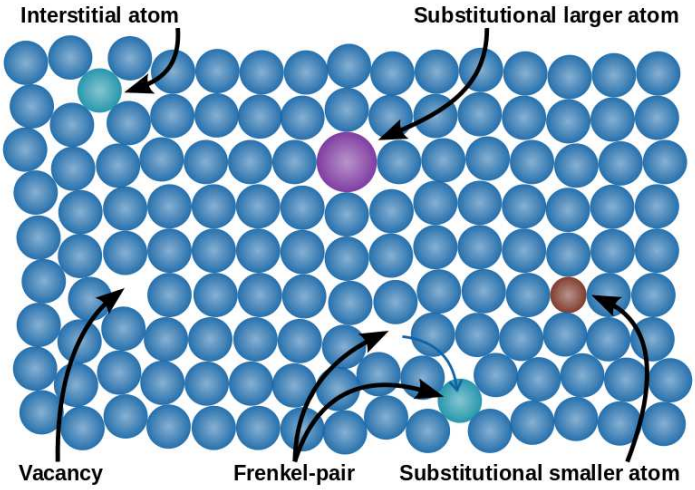

Figure 3.9: Point defect types in semiconductor crystal. Vacancies are empty lattice places where atom is missing. Interstitials are extra atoms between the actual lattice atoms. In Frenkel pair the lattice atom is displaced, forming a vacancy and an interstitial. Substitutional atoms are impurity atoms substituting an original lattice atom. Antisites can occur in compound lattices, where two atoms of different type have exchanged their positions (not illustrated in the figure).[60, 61]

The most common defects in undoped ZnO are oxygen vacancies, Zn interstitials and Zn vacancies. O vacancies are deep donors and have high formation energies in n-type ZnO and are therefore unlikely to form in significant concentrations, but among the defects that behave as donors, O vacancies have still the lowest formation energy. The formation energy is much lower in p-type ZnO. Thus, oxygen vacancies are a potential source of compensation in p-type ZnO.[62, 63]

Zn interstitials are shallow donors, but they have also high formation energies in n-type ZnO and are too mobile to be stable at room temperature. Zn interstitials are present in very low concentrations in n-type ZnO, but in p-type the formation energy is relative low. Zinc interstitials are also a potential source of compensation in p-type ZnO.[62, 63]

Zn vacancies are deep double acceptors and they act as compensating centers in n-type ZnO. They have also the lowest formation energy among the native point defects in n-type ZnO. On the other hand, Zn vacancies have exceedingly high formation energies in p-type ZnO, and therefore exist only in very low concentrations.[62, 63]

Other native defects, such as O interstitials, O antisites and Zn antisites, have considerably higher formation energies and under normal conditions they are not present in large concentrations. Oxygen interstitials can occur as deep acceptors at octahedral interstitial sites in n-type ZnO or as electrically neutral split interstitials in p-type materials. Oxygen antisites are acceptors and zinc antisites are shallow donors, but they are unlikely to be stable under equilibrium conditions.[62, 63]

Unlike in other semiconductors, hydrogen acts always as a donor in ZnO. Interstitial hydrogen is tightly bound to an oxygen atom in ZnO, forming an OH bond with a length of about 1.0 Å. In n-type ZnO, the formation energy for hydrogen is low (only 1.56 eV) and in p-type ZnO, incorporation of hydrogen is even more favorable. This may be beneficial for obtaining p-type ZnO; incorporation of hydrogen during growth may increase acceptor solubility and suppress formation of compensating defects. Hydrogen is present in all growth methods and it can easily diffuse into ZnO in large amounts due to its large mobility.[2, 62]

Experimental results about point defects in ZnO obtained by low-temperature photoluminescence are presented in the Section 3.3.5.

3.3.4 Doping

The main problem with ZnO optoelectronic applications is a phenomena called ambipolar (or unipolar) doping; doping of one type (e.g. n-type with shallow donors) is easily possible up to high densities, while the opposite type (in this case p-type by shallow acceptors) is hardly achievable. This problem is found frequently for wide bandgap materials.[1] Undoped wurtzite ZnO shows intrinsic n-type conductivity with typical carrier concentrations of about $10^{16} \sim 10^{18}$ cm^{-3}.[43] Although it is experimentally known that unintentionally doped ZnO is n-type, whether the donors are Zn_i and V_0 is still controversial. It has also been suggested that the n-type conductivity of unintentionally doped ZnO films is only due to hydrogen (H), which acts as a shallow donor with an ionization energy about 30 meV. This assumption is valid since hydrogen is always present in all growth methods and can easily

diffuse into ZnO in large amounts due to its large mobility.[2]

When the impurities are introduced into otherwise perfect semiconductor crystal, additional energy levels are created in the energy band gap structure, usually within the bandgap. Donor impurity levels are usually located near the valence band minima and acceptor impurity levels near the conduction band maxima, as illustrated in Figure 3.10. Shallow acceptors and donors are impurities that require little energy to ionize; typically around the thermal energy or less. In other words their energy levels are close to the energy gap egde. Deep acceptors and donors require energies larger than the thermal energy to ionize and therefore only a fraction of the impurities present in the semiconductor contribute to free carriers. Deep impurities which are more than five times the thermal energy away from either band edge are very unlikely to ionize. Such acceptors and donors can be effective recombination centers in which electrons and holes fall and annihilate each other. Such deep impurities are also called traps.[51]

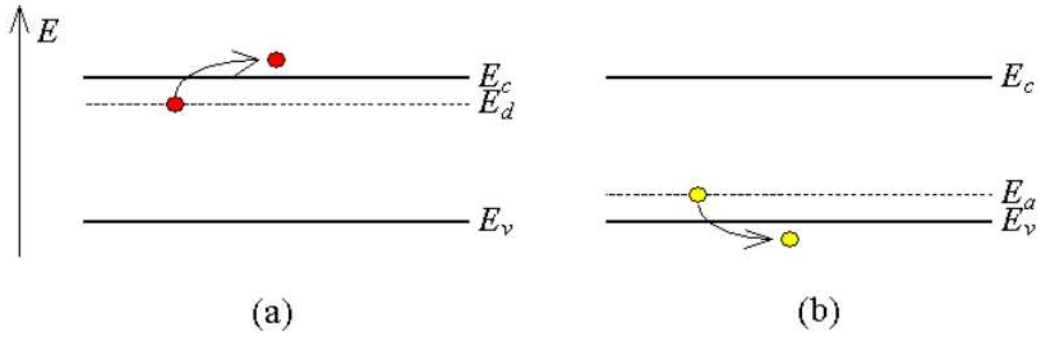

Figure 3.10: Ionization of (a) a shallow donor and (b) a shallow acceptor. The energy levels of doping impurities (E_d and E_a) are located close to the band gap edges.[64]

n-type doping of ZnO is relatively simple compared to p-type doping; Zn or O have to be substituted with atoms that have one electron more in the outer shell than the atom which they replace. The group III elements Al, Ga, and In are shallow and efficient donors on Zn cation sites, resulting in high-quality, highly conductive n-type ZnO films.[2] Electron concentrations beyond 10^{20} cm^{-3} are obtained in ZnO:Al and ZnO:Ga. The other possibility for n-type doping is using group VII elements on the O anion site. Though this combination is known to be very efficient, e.g. for ZnSe:Cl, it has been

less investigated for ZnO.[1] n-type doping of ZnO is developed very well. Such films are successfully used in various applications as n-type layers in light-emitting diodes as well as transparent Ohmic contacts.[2]

The difficulties in p-type doping arise from a variety of causes; dopants may be compensated by low-energy native defects, such as Zn_i or V_O, or background impurities (H). Low solubility of the dopant in the host material is also another possibility. Deep impurity level can also be a source of doping problem, causing significant resistance to the formation of shallow acceptor level.[2]

According to the n-type doping rules, the group I elements Li, Na, or K would be suitable acceptors on Zn sites and the group V elements N, P and As on O sites for the p-type doping of ZnO. However, many of the group I dopants form deep acceptors and do not contribute significantly to p-type conduction. They tend to occupy the interstitial sites, partly because of their small atomic radii, rather than substitutional sites and therefore act mainly as donors instead. Moreover, significantly large bond lengtsh of Na and K compared to the ideal Zn-O bond length induces lattice strain, increasingly forming native defects such as vacancies which compensate the dopants. The group V elements are believed to be the most promising dopants for p-type doping, although theory suggests some difficulty in achieving shallow acceptor level. Both P and As also have large bond lengths and to avoid the lattice strain they are likely to form antisites, where two atoms of different type have exchanged their positions. The antisites are donorlike and provide yet another unwelcome possible mechanism for compensating acceptors. The best candidate so far for p-type doping in ZnO is N, because among the group V impurities N has the smallest ionization energy and it does not form antisites.[1, 2]

Another solution to p-type doping of ZnO could be codoping, i.e. using either two different acceptors simultaneously such as ZnO:N,As or ZnO:Li,N or combining even a moderate concentration of donors with a higher concentration of acceptors, e.g. in ZnO:Ga,N.[1]

3.3.5 Optical properties

The optical properties of a semiconductor are related to both intrinsic and extrinsic effects. Intrinsic optical transitions take place between the electrons in the conduction band and holes in the valence band, including excitonic effects due to the Coulomb interaction. Exciton is a bound state of electron and hole which are attracted to each other by the electrostatic Coulomb force.

Excitons are classified into free and bound excitons. In high-quality samples with low impurity concentrations, the free exciton can also exhibit excited states in addition to their ground-state transitions. Extrinsic properties are related to dopants or defects, which usually create discrete electronic states in the band gap, and therefore influence both optical absorption and emission processes. The electronic states of the bound excitons (BEs) depend strongly on the semiconductor band structure. Excitons can be bound to neutral or charged donors and acceptors. A basic assumption in the description of the bound exciton states for neutral donors and acceptors is a dominant coupling of the two identical particles in the BE states. For a shallow-neutral donor-bound exciton (DBE), for example, the two electrons in the BE state are assumed to pair off into a two-electron state with zero spin. The additional hole is then weakly bound in the net hole-attractive Coulomb potential set up by this bound two-electron composition. Similarly, shallow-neutral acceptor-bound excitons (ABEs) are expected to have a two-hole state derived from the topmost valence band and one electron interaction. These two classes of bound excitons are by far the most important cases for direct band gap materials. Other defect-related transitions could be seen in optical spectra, such as free to bound (electron-acceptor), bound to bound (donor-acceptor), and the so-called yellow/green luminescence. [2]

Defects and impurities relevant for the electron or hole conductivity form shallow donor or acceptor states and therefore the optical spectrum near the band gap is greatly affected by their incorporation into the lattice. The prevalence of several shallow donor impurities gives rise to narrow emission lines in the luminescence spectra of as grown n-type ZnO, originating from the radiative recombination of excitons bound to the shallow impurity states. These transitions can provide diverse information about the impurities, such as the charge state, chemical identity and dopant type. Despite the long lasting research on ZnO, these properties are not yet distinguished for all observable bound exciton emission lines. The presence of structural defects such as interstitials, vacancies, dislocations and stacking faults may create undesired radiative and non-radiative recombination channels, leading to the appearance of additional emission lines.[65]

The luminescence spectrum of ZnO covers almost the whole visible and near UV spectral range from 2.0 eV to 3.45 eV, as illustrated in Figure 3.11. The strongest luminescence is typically found near the band gap with particularly diverse emission lines at low temperatures, originating from the radiative recombination of free and bound excitons. The ZnO luminescence spectrum can be coarsely divided into four regions; green luminescence, lon-

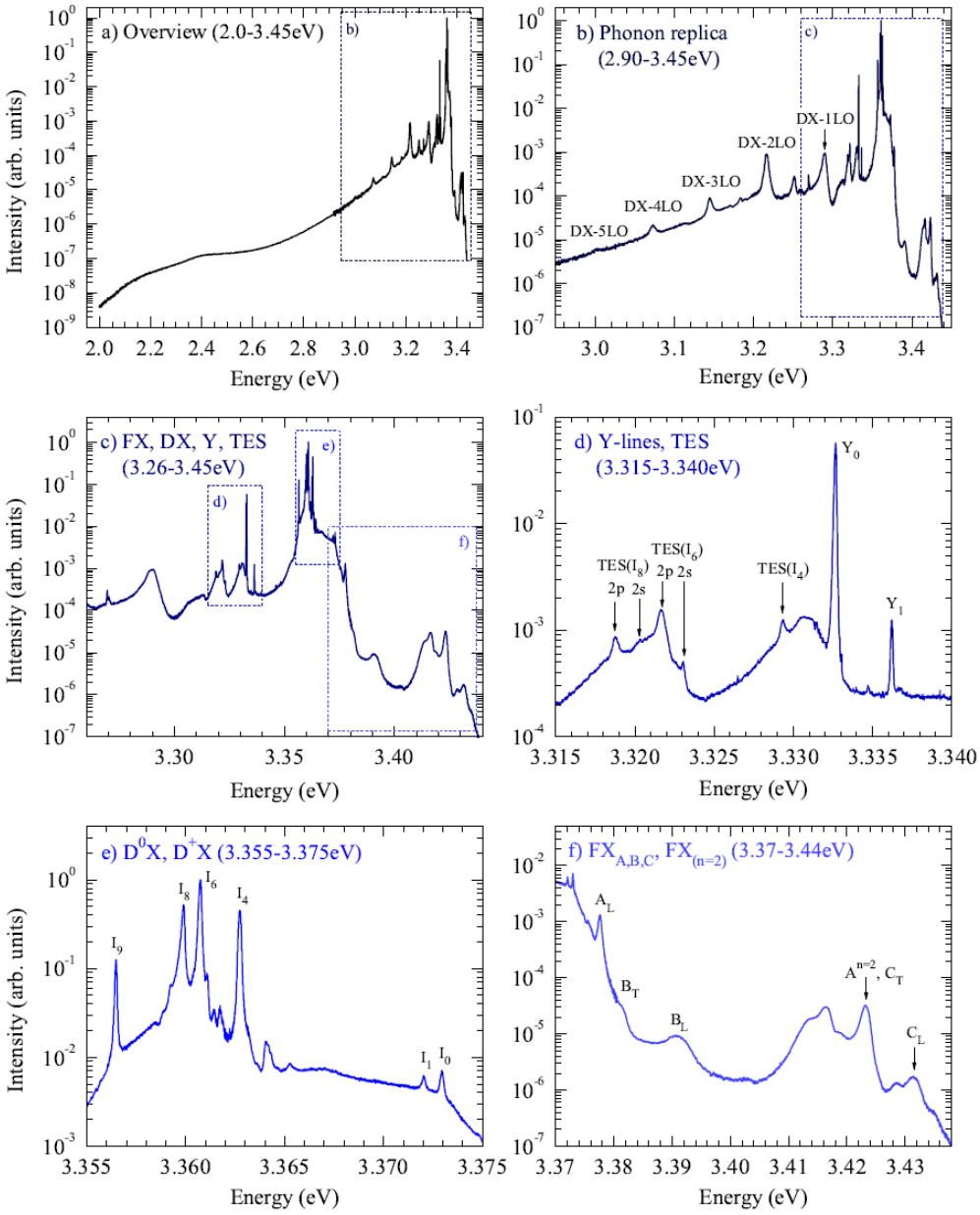

Figure 3.11: Photoluminescence spectra of a ZnO substrate at T=2 K. The selected areas are magnified in the specified graphs. (a) Overview spectrum (2.0-3.45 eV), (b) excitons and their phonon replicas (2.90-3.45 eV), (c) near band-edge luminescence including free exciton-polaritons (FX), donor (DX) and defect bound excitons (Y), two electron satellites (TES) and the first phonon sideband (1LO) of the DX (3.26-3.45 eV), (d) TES and Y lines (3.315-3.340 eV), (e) neutral (D^0X) and ionized donor bound excitons (D^+X) (3.355-3.375 eV), (f) free exciton-polaritons including holes from the A, B and C valence bands in the ground state (n=1) and excited states (n≥2) (3.37-3.44 eV).[65]

gitudinal optical phonon (LO) replica/two-electron satellite (TES), bound exciton and free exciton regions.[65] In the lower end of the spectum there is also some doping-related luminescence.

In the low energy range between 2.0 eV and 2.8 eV, a green luminescence (GL) band is commonly observed in ZnO with a maximum intensity at about 2.5 eV (Fig. 3.11 (a)). It consists of two overlapping peaks originating from deep copper acceptors and native point defects, such as oxygen and zinc vacancies. The copper related luminescence arises from the radiative recombination of excitons intermediately bound to copper impurities. In addition to the copper related luminescence, there is typically a structureless green emission band attributed to different transitions involving native point defects. It may strongly vary in intensity and exhibit one or two peak maxima at different energies in this spectral range, depending on the growth conditions and prevailing defect centers. The proposed point defects responsible for the green luminescence include oxygen vacancies V_O, zinc vacancies V_{Zn}, zinc interstitials Zn_i and antisites O_{Zn} resulting in band-acceptor (e,A), donor-band (D,h), donor-acceptor pair (DAP) and intracenter V_O (between two states of V_O) transitions.[2, 65] Doping ZnO with Li acceptor results in the yellow luminescence band with a peak at about 2.2 eV. In contrast to the GL band, the YL band decays very slowly after switching off the excitation source. The DAP-type transitions including a shallow donor and the Li acceptor dominate at low temperatures. After air annealing of undoped bulk ZnO at 700°C a red luminescence (RL) band emerges at about 1.75 eV in the PL spectrum. With increasing temperature, the RL band decays in the range from 15 to 100 K. The decaying of the RL band apparently causes the emergence of the GL band. This may be a result of competition for holes between the acceptors responsible for the GL and RL bands. At T>200 K, the GL band decays rapidly, so that the RL band is observed alone at room temperature.[2]

In the energy range between 2.9 eV and 3.3 eV the luminescence spectrum of ZnO consists of a multitude of longitudinal optical phonon (LO) replicas of the bound excitons with an energy separation of 71-73 meV (that is the LO-phonon energy in ZnO) (Fig. 3.11 (b) and (c)). If a sufficient amount of shallow acceptor states is present, donor-acceptor pair (DAP) transitions may also appear in this region. For example, a nitrogen related shallow DAP band occurs around 3.235 eV followed by at least two phonon replicas. In addition to the LO replica and DAP emission, luminescence features between 3.315 and 3.340 eV are commonly observed in ZnO samples (Fig. 3.11 (d)). They can be attributed to the recombination of excitons bound to extended structural defects. The remaining luminescence of the upper part of this region (3.32-3.34 eV) is related to two-electron satellite (TES) transitions

of the dominant bound excitons. These lines appear if the bound exciton recombination leaves the neutral donor in an excited state instead of the ground state. The transition energy is less than the DBE energy by an amount equal to the energy difference between the first excited and ground states of the donor.[2, 65]

The strongest luminescence with several sharp emission lines is observed between 3.348 eV and 3.375 eV (Fig. 3.11 (e)). They originate from the radiative recombinations of excitons bound to impurities. The impurity centers can exist in the neutral and ionized charge state. The ionized impurity bound excitons are located at higher energies than the neutrally charged ones. In high-quality bulk ZnO substrates the neutral shallow DBE often dominates because of the presence of donors due to unintentional (or doped) impurities and/or shallow donorlike defects. In samples containing acceptors, the ABE is observed. So far, up to 20 different bound exciton transitions were reported, but the identification of specific bound exciton lines is complicated by several effects. Exciton excited states may occur at the same or close to the energies of other bound excitons in the ground state and mistakenly be identified as such. Another challenge is the distinction between donor and predicted acceptor bound excitons, since the range of their localization energies could overlap between 16 and 25 meV. The absolute position of the emission or absorption lines may also be shifted because of different strain levels in ZnO samples, impeding the comparability of the exciton emission in different samples.[2, 65]

Above the energies of the bound excitons, the free exciton luminescence is observed between 3.375 eV and 3.440 eV (Fig. 3.11 (f)). As already described in Section 3.3.2, the wurtzite ZnO valence band is split into three bands due to the influence of crystal-field and spin-orbit interactions (Figure 3.7). The near-band-gap intrinsic absorption and emission spectrum is therefore dominated by transition from these three valence bands. The related free-exciton transitions from the conduction band to these three valence bands or vice versa are usually denoted by A (also referred to as the heavy hole), B (also referred to as the light hole), and C (also referred to as crystal-field split band).[2, 65] The excitonic binding energy for all three exciton series resulting from the transitions from the A, B and C valence bands into the conduction band is roughly 60 meV.[1] It is a large value compared to other wide-band-gap semiconductors and it makes ZnO useful in efficient lasing devices based on stimulated emission due to the recombination of excitons also at room temperature. The coupling of excitons with the electromagnetic field results in the formation of exciton-polaritons, altering the dispersion relation of the excitons. In addition to excitons with holes from the A valence band, also B and C exciton-polaritons are visible in high sensitivity PL studies. The

luminescence of these features is up to six orders of magnitude weaker than the donor bound exciton emission, requiring sufficiently sensitive detection electronics. In addition to the ground state excitons (n=1), also the excited states (n≥2) of the A and B excitons are observed. [2, 65]

3.4 ZnO thin film growth methods

There are many methods that have been employed to grow ZnO films, such as metalorganic chemical vapor deposition (MOCVD)[3], molecular beam epitaxy (MBE)[4], sputtering[6], pulsed laser deposition (PLD)[5] and atomic layer deposition (ALD)[14]. Sapphire (Al_2O_3) has been conventionally the most popular substrate for all the ZnO growth methods because of its low cost, availability as large-area wafers and its wide energy-band gap despite its poor structural and thermal match to ZnO[2]; the lattice mismatch is about 18 %[66]. Therefore more suitable substrates are also applied, such as YSZ (lattice mismatch about 10%)[14], silicon (lattice mismatch about 40 %[66]), SiC (lattice mismatch about 5 %)[66] and GaN (mismatch is about 1.8 %[67]). The most common growth methods are briefly introduced below.

3.4.1 Metalorganic chemical vapor deposition (MOCVD)

In MOCVD (metalorganic chemical vapor deposition, also known as metalorganic vapour phase epitaxy, MOVPE) the reactant gases are combined at elevated temperatures in the reactor to cause a chemical reaction, resulting in the deposition of materials on the substrate in the gas phase at moderate chamber pressure (from 10 mbar to 1 bar). Gas is introduced via devices known as bubblers, where a carrier gas (such as nitrogen or hydrogen) is bubbled through the metalorganic liquid, which picks up some metalorganic vapour and transports it to the reactor. The vapor pressure of the metal organic source is an important factor in MOCVD, because it determines the concentration of the source material in the reaction and the deposition rate. The typical growth temperature for epitaxial ZnO is between 250-650°C.[2, 9]

3.4.2 Molecular beam epitaxy (MBE)

Molecular beam epitaxy (MBE) requires high or ultra-high vacuum (10^{-6}-10^{-15} bar).The ultra high vacuum environment and the absence of carrier

gases result in the highest achievable purity of the grown films. In solid-source MBE elements are heated in separate Knudsen cells until they begin to sublime. The gaseous elements condense on the wafer, where they may react with each other. Computer controlled shutters allow precise control of the thickness of each layer, down to a single layer of atoms. Providing the oxygen source for ZnO growth is more complicated; the high molecular bond strength of diatomic oxygen limits the thermal dissociation of molecules into atoms and prevents the use of simple thermal gas cracking. Available methods for breaking the molecules are radio frequency plasma, radical sources, electron cyclotron resonance sources and a simple ozone source. The typical growth temperature for epitaxial ZnO is between 350-650°C.[2, 9]

3.4.3 Pulsed laser deposition (PLD)

In pulsed laser deposition (PLD) a high-power pulsed laser beam is focused inside a vacuum chamber to strike a target consisting of the deposition material. This material is vaporized from the target into a plasma plume and thereby deposited as a thin film on a typically hot substrate. The stoichiometry of the material is preserved in the interaction. The process can occur in ultra high vacuum or in an ambient gas, such as oxygen in the case of ZnO. The main processing parameters of PLD such as substrate temperature, background gas pressure and laser intensity play important role on the growth and properties of ZnO films. PLD allows the growth of thin films in reactive oxygen pressure (from 10^6 to 1 mbar) with the same composition as that of the target. This makes PLD particularly well suited for growing thin oxide films. The temperature range for epitaxial growth is between 300-800°C. The best layer quality in achieved with temperatures higher than 750°C, but using the ultraviolet-assisted PLD technique (UVPLD) the equal layer quality is achieved with at least 200°C lower temperatures. In UVPLD an UV source provides in situ irradiation with UV photons during the PLD process.[2, 9]

3.4.4 Sputtering

In sputtering a solid target material is bombarded by energetic particles and material is then ejected (sputtered) from the target and afterwards deposited on a substrate in the vicinity. The process is carried out in a closed chamber which is pumped down to a vacuum before deposition. In RF-sputtering (radio frequency) an AC-voltage is applied to the target. In one phase, ions are accelerated towards the target surface and sputter material. In the other phase, charge neutrality is achieved. As a result also sputtering of non-

conducting material is possible. The properties of the deposited thin films differ according to sputtering conditions, pressure, temperature, components of the target and atmosphere, distance of substrates and films growth ratios. In conventional sputtering methods it is difficult to optimise the deposition conditions. The electron cyclotron resonance (ECR) sputtering method has been developed to overcome this difficulty. The ECR plasma is generated by microwaves with a magnetic field set-up by the ECR condition. The process can be easily controlled independently of the generation of plasma. High quality epitaxial ZnO films have been deposited on the sapphire substrates at 250-550°C by ECR sputtering. The conventional methods require growth temperatures of 400-600°C for epitaxial ZnO growth.[2, 9]

3.4.5 Atomic layer deposition (ALD)

Atomic layer deposition (ALD) process is discussed detailed in Chapter 2 and the ALD growth of epitaxial ZnO is presented in the Chapter 4. ALD is a film deposition technique that is based on the sequential use of self-terminating gas-solid (chemical) reactions in pressures of 0.1-10 mbar. The growth of layers by ALD consists of repeating four steps: self-terminating reaction of the first precursor A, purge to remove the nonreacted reactants and the gaseous reaction by-products, self-terminating reaction of the second precursor B and again purge. These steps constitute a reaction cycle that is repeated until the desired amount of material has been deposited. The ALD method is a variant of the chemical vapor deposition (CVD) technique with alternate supply of two precursors. The use of self-terminating reactions means that ALD is a surface-controlled process, where process parameters other than the reactants, substrate, and temperature have little or no influence. Because of the surface control, ALD-grown films are extremely conformal and uniform in thickness.[22] Epitaxial ZnO ALD growth requires growth temperature of about 300°C.[14]

3.5 ZnO thin film applications

Due to the wide direct band gap, the most common applications for ZnO are in laser diodes and light emitting diodes (LEDs). Some optoelectronic applications of ZnO overlap with that of GaN, which has a similar bandgap. Compared to GaN, ZnO has a larger exciton binding energy (60 meV vs. 25 meV), resulting in bright room-temperature emission from ZnO. ZnO is the most promising candidate in the field of random lasers to produce an electronically pumped UV laser source. However, the biggest issue with the

future optoelectronic applications of ZnO is to achieve high, stable and reproducible p-doping.[1] Because of its wide bandgap, ZnO is also transparent in the visible part of the light spectrum. Highly n-doped ZnO:Al thin films are used as a transparent conducting oxide (TCO). The constituents Zn and Al are much cheaper and less poisonous compared to the generally used indium-tin oxide (ITO). Other applications are the front contacts to solar cells and liquid crystal displays. Transparent thin-film transistors (TTFT) can be produced using ZnO due to its its high optical transmittivity and high conductivity. In the version of field-effect transistors a p-n junction is not even needed, avoiding the problem of the p-type doping of ZnO. Some of the field-effect transistors even use ZnO nanorods as conducting channels.[1, 68] Al-doped ZnO thin films are also used in the production of energy-saving or heatprotecting windows; a coating with TCO results in a glass which lets the visible part of the spectrum in but either reflects the IR back into the room (energy saving) or does not let the IR radiation into the room (heat protection), depending on which side of the window has the TCO coating.[39]

Other properties of ZnO favorable for electronic applications include its stability to high-energy radiation and to wet chemical etching. The radiation hardness of ZnO to MeV proton irradiation makes ZnO a suitable candidate for space applications. Since the surface conductivity of ZnO can be strongly influenced by various gases, it is used in gas sensor applications.[1, 57] Other promising areas of application for ZnO are acoustic wave devices and other piezoelectrical applications due to large electromechanical coupling in ZnO. ZnO appears to be well suited also for producing nanostructures, which may be used for devices such as biosensors and photodetectors. A significant part of the recent research in the field of ZnO-based devices and applications deals with ZnO nanostructures (nanowires, nanobelts etc.) and their integration with the mainstream semiconductor materials such as Si, GaN, and organic semiconductors. ZnO nanowires have attracted a lot of attention due to their good charge carrier transport properties and high crystalline quality. Such 1-D systems have unique properties that make them potentially attractive for nanoscale devices.[68]

Chapter 4

Sample preparation

This chapter presents the experimetal procedures done for this work: GaN template growth and cleaning, ZnO growth process by ALD and annealing process performed after the film characterization.

4.1 Template preparation

Zinc oxide was grown on c-plane GaN/sapphire templates. GaN layers were grown on commercial sapphire substrates by metalorganic chemical vapor deposition (MOCVD). The basic characteristics of the MOCVD method are described in Section 3.4.1. Ammonia (NH_3) and trimethylgallium (TMGa) were used as the N and Ga sources, respectively. The growth temperature was 1050°C and the chamber pressure was 270 mbar. First a 2 μm thick GaN layer was grown on sapphire with a standard two-step method [69], that includes a thin nucleation layer (about 50 nm) grown at low temperature (530°C) and about 2 μm thick buffer layer grown at 1050°C, resulting in flat GaN surface. Then an additional 2 μm thick GaN layer was grown on the buffer layer. The total thickness of the GaN layers was about 4 μm.

4.2 Cleaning

The GaN/sapphire templates were cleaned by dipping them in deionized water and 2-propanol and then blow dried with N_2 gas for removing particles from the sample surface before the ALD deposition of ZnO.

4.3 ZnO growth process by ALD

Zinc oxide was deposited by a flow type ALD apparatus (Beneq TFS 500) with a continuous nitrogen carrier gas flow through the reactor. The reactor pressure during the growth was about 1.8 mbar. Diethylzinc (DEZn, $(C_2H_5)_2Zn$) and water vapour (H_2O) were used as Zn and O precursors, respectively. DEZn and H_2O react via double-exchange chemical reaction:

$$\begin{aligned} &C_2H_5 - Zn - C_2H_5 + H_2O \\ &\quad \rightarrow ZnO + 2C_2H_6 \end{aligned} \tag{4.1}$$

where the reaction products are zinc oxide and ethane.[70] One cycle consisted of one DEZn pulse followed by purge with nitrogen gas and one H_2O pulse followed by nitrogen purge. DEZn pulse length was 500 ms and purge time 2 s. H_2O pulse length was 250 ms and purge time 2 s. Both precursors were held at 20°C, and the growth chamber temperature was varied from 280°C to 325°C (280°C, 290°C, 300°C and 325°C). The number of cycles for each sample was 1000. In theory this corresponds to a layer thickness of approximately 60 nm, but the XRD measurements reveal that the actual thickness differs from that. The ALD growth window for ZnO growth using DEZn and H_2O as precursors is about between 100-180°C[12], so the differences in the growth rate in our study are explained by various effects. In addition, a thicker layer with 10 000 cycles was grown for the positron annihilation measurement.

The maximum growth temperature was chosen to be 325°C because the complete thermal decomposition temperature of DEZn is around 360°C and the temperature corresponding to the half-decomposition is estimated to be about 330°[71]. This limits the maximum practical growth temperature, because the ALD reaction remains incomplete if DEZn ions are prematurely dissociated before the surface reaction with the substrate[21].

4.4 Annealing

By annealing it is possible to modify the film structure after the growth process. Annealing causes crystallization and in case of amorphous films the film structure can be transformed to polycrystalline film. Annealing can remove defects and enhance the film quality, and thereby also improve optical and electrical properties of the film. Oxygen annealing of oxide films can result in more stoiciometric films. Other applications of annealing are

intrinsic stress liberation of thin films and dopant activation. Annealing can be done in a traditional gas furnace, when the annealing time is typically from tens of minutes to hours. Another option is rapid thermal annealing (RTA), where the sample is heated in few seconds from room temperature to target temperature using high-intensity lamps or lasers. The RTA annealing times are typically only from minutes to tens of minutes.[72]

There are some reports about distinct improvement of ALD ZnO film quality due to annealing in N_2 [16, 18, 73–75] and O_2 [16, 17, 20, 76–78] environments in temperature range of 300-1000°C by both gas furnace [16–18, 21, 73, 76–78] and RTA [16, 19, 20, 74, 75]. Annealing has reported to enhance the structural and optical properties, but most of the applied templates are sapphire [16, 17, 20, 73, 74, 76–78] or silicon [18, 19, 21] and in only one case GaN [75]. Also in only four cases the ALD ZnO growth temperature is higher than 200°C [16, 17, 20, 21] and in one of them the zinc precursor is zinc acetate [17], affecting essentially on the growth parameters. There are no reports about annealing clearly epitaxial ALD ZnO samples on GaN template.

In this work the same samples (ALD grown ZnO on GaN template at 280-325°C using DEZn as zinc precursor) were annealed in 1000°C oxygen gas furnace for one hour. The annealing temperature was chosen to be lower than the GaN growth temperature, but high enough to produce effective annealing results.

Chapter 5

Thin film characterization

This chapter presents the thin films characterization methods applied in this work. ZnO thin films were analyzed with scanning electron microscope (SEM), atomic force microscopy (AFM), X-ray diffraction (XRD) and photoluminescence (PL) measurements to analyze the effect of the growth temperature on the crystalline quality and the defect structure of the layers. One sample was also studied with positron annihilation spectroscopy (PAS). The samples were characterized with SEM again after annealing.

5.1 Scanning electron microscope

The resolution of conventional microscopes has a fundamental limit near the wavelength of the visible light. Therefore a shorter wavelength is required to study samples with details in the nanometer scale. Scanning electron microscopy utilizes a well focused low energy electron beam accelerated towards the sample surface. The beam electrons interact with atoms of the sample, producing ia. secondary and back scattered electrons. Secondary electrons are emitted by atoms excited by the electron beam, whereas back scattered electrons are beam electrons that are reflected from surface atoms by elastic scattering. They are both commonly used for imaging samples: secondary electrons are most valuable for showing morphology and topography on samples, whereas back scattered electrons are most valuable for illustrating contrasts in composition in multiphase samples. Large area of the surface is irradiated by rapidly sweeping the focused beam on the surface and the image is constructed from the position of the beam and the intensity of the detected electrons. SEM is capable to obtain a resolution of only a few nanometers, depending mostly on the beam focus spot size.[79, 80]

In this work the sample surfaces were characterized with Zeiss Supra 40 scanning electron microscope (SEM) with an in-lens detector. The acceleration voltage of the electron beam was 10 kV and magnification 100 000 x, except with annealed samples the magnification was 10 000 x.

5.2 Atomic force microscope

Atomic force microscopy generates a topological map of the sample surface on an atomic scale. AFM employs a small cantilever with a very sharp tip at its end that in brought into close proximity of the sample surface. The tip may come into direct or close contact with the surface, so that they may both interact with each other through attractive or repulsive forces (e.g. electrostatic and van der Waals force), depending on the proximity of the tip to the surface. The tip is raster-scanned across the plane of the surface. During scanning the probe experiences deflections perpendicular to the plane in response to interactions between the tip and the surface. The vertical motions of the tip are controlled by piezoelectric ceramic components and a feedback mechanism adjusts the tip-to-sample distance (and the force between them) to maintain constant. The tip movements are monitored electronically and transferred to computer to generate the three-dimensional surface image. AFM can be operated in contact, semi-contact (or "tapping") and non-contact mode, name referring to the proximity of the tip to the surface. Contact mode is the most common mode, but because of the direct contact the tip can deform the sample surface and create false image. In semi-contact mode the tip periodically touches or taps the surface of the sample. It provides the best resolution and it can be used to scan fragile and soft samples. Non-contact mode can be applied even to fluid surfaces, but the resolution is lower because of the weak forces between the tip and the surface.[81, 82]

In this work AFM measurements were done to determine the topography of the sample surfaces by scanning them with Ntegra scanning probe microscope in semi-contact mode. The scanned area was $1\mu\text{m}\times1\mu\text{m}$, and the RMS roughness and its standard deviation were determined by measuring all the samples each from 4 points and calculating the statistical values.

5.3 X-ray diffraction

X-ray diffraction (XRD) is a powerful non-destructive technique for characterizing crystalline materials. It provides information on structures, phases, preferred crystal orientations (texture) and other structural parameters, such as average grain size, crystallinity, strain and crystal defects. The crystalline sample is bombarded with x-ray beam from different angles by rotating the sample mounted in goniometer in the beam. X-ray diffraction peaks are produced by constructive interference of a monochromatic beam of x-rays scattered at specific angles from each set of lattice planes in a sample. The peak intensities are determined by the distribution of atoms within the lattice. The resulting diffraction patterns of reflections are measured and recorded.[83, 84]

The principle of X-ray diffraction analysis is the Bragg law:

$$n \cdot \lambda = 2 \cdot d \cdot sin\theta \tag{5.1}$$

where the integer n is the order of the corresponding reflection (can be assumed 1), λ is the X-ray wavelength, d is the spacing between the planes in the atomic lattice and θ the angle between the incident ray and the scattering planes, as seen in Figure 5.1. By measuring the angle θ, the lattice interplanar spacing d can be calculated.[85]

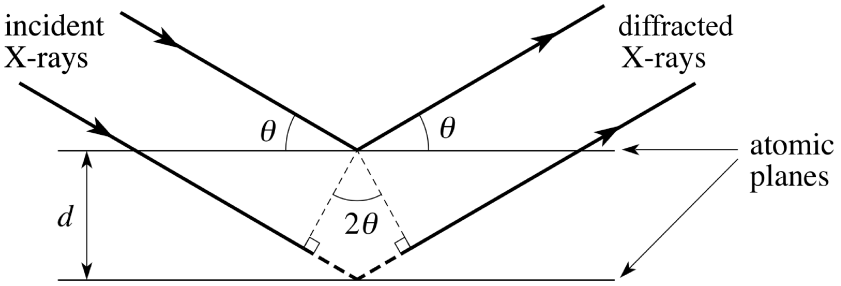

Figure 5.1: X-rays scattering from lattice planes, following the Bragg law.[86]

The interplanar spacing d can then be used to determine the lattice parameters a and c by knowing the coordinates of the diffraction plane (Miller indices (hkl)). The correlation between the lattice parameters and the interplanar spacing in the hexagonal lattice (such as ZnO and GaN) is defined as [85]

$$d_{hkl} = \sqrt{\frac{3}{4\{\frac{h^2+k^2+hk}{a^2} + \frac{3l^2}{4c^2}\}}} \tag{5.2}$$

With samples having several layers or other complex structures the XRD analysis are naturally more complicated, but XRD is effective analyzing method also for them.

In this work the high resolution XRD measurements were done using Phillips X'pert Pro diffractometer operating at $CuK_{\alpha 1}$ wavelength (λ = 1.540560 A) with measurement assembly consisting of Ni and Cu attenuators, X-ray mirror, Soller slit (0.04 rad) and divergence slit with 1/32° fixed aperture at incident beam setup. The reflected beam was collected using thin film collimator, 0.04 radian Soller slit, flat graphite crystal monochromator and scintillation detector assembly. A programmable divergence slit with an automatic aperture set was used to keep a 10 mm beam width in each angle. The reflected beam was measured by using programmable anti-scattering slit collecting radiation from the 10 mm beam area to the scintillation detector. XRD ω-2θ scans and high-resolution reciprocal space maps were measured to define the crystalline structure of the ZnO layers. The ω-2θ scan (scanning of incident and diffracted beam angle, also called "rocking curve") shows the diffractions peaks from the lattice planes over the specified angle distribution. Reciprocal space maps consist of series of ω-2θ scans that are combined in one two-dimensional map and they give additional, visualized information about the lattice structure.

5.4 Photoluminescence

In photoluminescence electron-hole pair excitation by incident photons induces light emission. Typically an intense laser beam is focused on the sample to create electron-hole pairs. When these electrons and holes recombine, the resulting photons are collected and directed to a photo-sensitive detector. The spectrum of the emitted photons is measured, giving information of the electron band structure of the material. At low measurement temperatures (only few degrees of K) the non-radiative recombination centers are frozen, so the radiative recombination reinforces. When the temperature decreases, also the peak widening caused by thermal movement decreases, so it is then possible to distinguish also narrow peaks located close to each other. Excitons have a certain binding energy and if the thermal movement exceeds it, the excitons decay. Therefore excitonic effects are more efficient at low tem-

peratures, while at higher temperatures the non-radiative processes become dominant. This has been termed as thermal quenching.[80, 87]

In this work the optical properties of the ZnO layers were studied with PL measurements by using an ultraviolet light emitted from a 325 nm He-Cd laser with standard lock-in techniques at low temperature (9 K). The setup consisted of the excitation laser, a focusing lens (focal length $\approx$ 35 mm), a semi-transparent mirror, an optical fiber and a detector consisting of a photomultiplier tube and a monocromator. The laser beam was focused on the sample, where it excited electron-hole pairs that recombined emitting light. The light was directed to an optical fiber which lead the light to the detector. The detector can detect emission wavelengths between 200-1100 nm, with approximately 1 nm accuracy. The spectrum was recorded by a computer to analyze the data, and the total PL intensity was obtained by integrating the total area of the peak.

5.5 Positron annihilation spectroscopy

In positron annihilation spectroscopy positrons are accelerated towards the sample. When a positron penetrates into the material, it can be trapped by certain kinds of defects in the lattice. A suitable defect introduces a potential well for the positron to localize. After a time, positron-electron annihilation occurs and two γ photons with peak energy of roughly at 511 keV are emitted to opposite directions. From the γ radiation, the type and concentration of the possible defects can be determined. The measurements are based on positron lifetime in the material and the shape of the spectrum of the γ photons created in the annihilation process.[88]

Positron lifetime spectroscopy and Doppler broadening are the most commonly used measurements when utilizing positron annihilation. A positron entering a defect free crystal has an average lifetime, typical of the material, before annihilating with an electron. Furthermore, depending on the momentum of the electron, the annihilation produces a certain shape of radiation spectrum. However, if there is a defect present in the crystal, the positron wave function can be localized, effectively trapping the positron. [94] When the positron gets trapped, the average lifetime before annihilation is altered. Also, annihilating electrons in the defect have different momentum values compared to electrons in a perfect lattice. These changes produce lifetime and Doppler broadening values of the gamma spectrum typical for the defect.[89]

In this work positron annihilation spectroscopy was applied to analyze the nature and concentration of point defects in the ZnO film. For this a thick (600 nm) layer of ZnO was grown with 10 000 cycles at 300°C (whereas the other samples had 1000 cycles). Doppler broadening of the positron-electron 511 keV annihilation line was measured using two high-purity Ge detectors and a variable-energy positron beam allowing for depth-resolved studies of thin film samples. Typically, the shape change is characterized with two lineshape parameters, which can be obtained by comparing two different regimes of the perfect lattice spectrum and the defect altered spectrum. The parameters are usually denoted S and W, determined as fractions of positrons annihilating with low ($\mid p_L \mid < 0.4$ atomic units (au)) and high momentum electrons (1.5 au $< \mid p_L \mid < 3.9$ au), respectively [95]. p_L is the longitudinal momentum component of the electron-positron pair in the direction of the 511 keV annihilation photon emission. The difference can then be defined as the area between the curves at the peak (S) and the tail (W), as shown in Figure 5.2. The type and the concentration of the point defect can usually be determined from S and W parameters [79, 64].

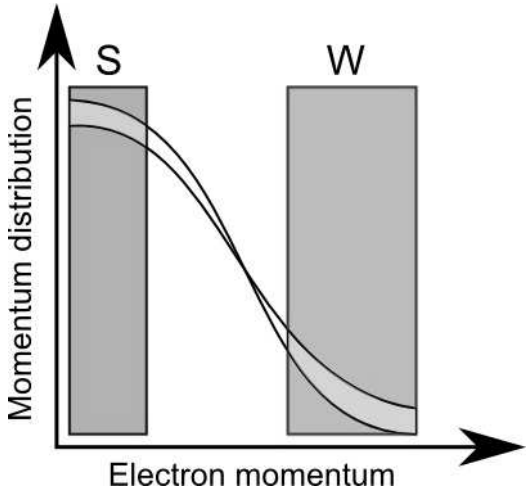

Figure 5.2: Illustration of obtaining the S and W parameters from the PAS measurement.[80]

Chapter 6

ALD growth of epitaxial ZnO

This chapter presents the basic characteristics of epitaxial growth of ZnO by ALD and the experimental results of this work which were also partly published in Journal of Crystal Growth [90].

6.1 Introduction

Epitaxy refers to the process of growing thin crystalline layers on a crystal substrate. In epitaxial growth there is a precise crystal orientation of the film in relation to the substrate. Epitaxy of the same material, such as ZnO film on ZnO substrate, is called homoepitaxy, while epitaxy where the film and substrate material are different is called heteroepitaxy. In homoepitaxy the substrate and film will have the identical structure (if the growth temperature is high enough), but in heteroepitaxy the substrate have to usually have the same lattice structure and similar lattice parameters as the growing film.[91]

ALD grown epitaxial ZnO has some supreme features such as the thickness control, layer uniformity and scalability for fabrication of modern semiconducting devices with 3D architecture.[8] The growth temperature is also lower than with most of the other methods [9], making it useful for many low-temperature applications.[8, 10] There are some promising applications for epitaxial ZnO films is in the fields of optics and optoelectronics. Using ALD to deposit epitaxial ZnO films can be particularly valuable for so-called multilayer interference mirrors that are used in X-ray optics.[92] This is due to the need for layered structures with highly precise layer thicknesses that can be fabricated relatively easily with ALD. The high quality of the ZnO films obtainable by ALD also makes the technique suitable for stimulated

emission applications, where the epitaxial ZnO films can be used in photonic devices in the UV range.[74]

6.2 Precursors

The most common ALD precursors for ZnO growth are diethylzinc (DEZn, $(C_2H_5)_2Zn$) and H_2O. Their threshold temperature for epitaxial growth is about 300°C. The complete thermal decomposition temperature of DEZn is around 360°C and the temperature corresponding to the half-decomposition is estimated to be about 330°[71], setting limitations for growth temperature selection because the ALD reaction remains incomplete if DEZn ions are prematurely dissociated before the surface reaction with the substrate.[21] DEZn and H_2O can be used to deposit ZnO films at considerably lower temperatures than the other precursor options, even at room temperature.[11]

There are also other less frequently used options for precursors in ALD ZnO growth. For zinc precursor are used also dimethylzinc (DMZn, $Zn(CH_3)_2$) [8], zinc chloride ($ZnCl_2$) [93], zinc acetate ($Zn(CH_3COO)_2$) [94] and elemental Zn gas [93]. For oxygen precursor selection there are also ozone (O_3) [95], nitrous oxide (N_2O) [96] and oxygen gas [93].

When DEZn is replaced by its methyl analogue dimethylzinc, higher GPC is obtained due to the smaller size of DMZn [13], having roughly the same epitaxial threshold temperature with DEZn.[8] With zinc chloride and oxygen gas epitaxial growth is achieved on both sapphire and GaN at temperature range 450-550°C.[93, 97] Resistivity is higher in the films grown from zinc acetate than in the films grown from DEZn.[17] Ozone is reported to accomplish improved material properties at lower growth temperatures, but in the temperature range of epitaxial growth the strong oxidative power of O_3 causes deterioration in the electrical properties including resistivity, carrier concentration, and mobility.[98] Process combining elemental precursors Zn and oxygen gas resulted in 3D growth with extremely low growth rate.[93]

6.3 Requirements for epitaxial growth

ALD growth of epitaxial ZnO requires usually relative high growth temperature (about 300°C using DEZn and H_2O as precursors [66]) and a hexagonal substrate. In ALD the chamber pressure has no reported effect on the epitaxial layer quality.

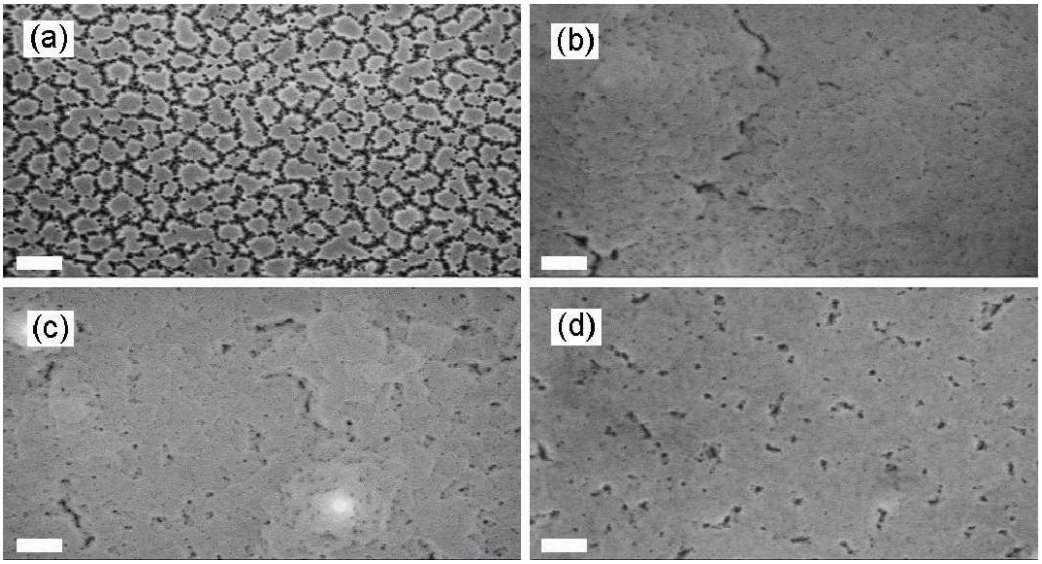

Figure 6.1: SEM images of ZnO surfaces with growth temperature of (a) 280 °C (b) 290 °C (c) 300 °C and (d) 325 °C. The scale bars correspond to 100 nm.[90]

6.3.1 Temperature

The threshold temperature for two dimensional growth of ZnO is found to be about 290 °C, when using DEZn and H_2O as precursors.[90] Figure 6.1 illustrates the effect of the increasing growth temperature on the film surface flatness for ALD grown ZnO on GaN around the threshold temperature of epitaxial growth.[90] The SEM images show that in the sample grown at 280°C (a) the surface structure seems consist of partially merged grains with thick and clearly distinctive grain boundaries, whereas the sample growth at 290°C (b) shows already clearly flatter surface morphology. The surface of the sample grown at 325°C (d) is completely flat with no 3-dimensional structures.

The non-epitaxial growth of ZnO by ALD has a ALD growth window about between 100-180°C, as seen in Figure 6.2. The growth rate is 1.8-1.9 Å per cycle inside the window.[12] Because the threshold temperature for epitaxial ZnO growth is considerably higher, the growth rate of epitaxial ZnO is therefore lower than in the growth window. The ALD growth limiting phenomenas outside the growth window are discussed in Section 2.1.

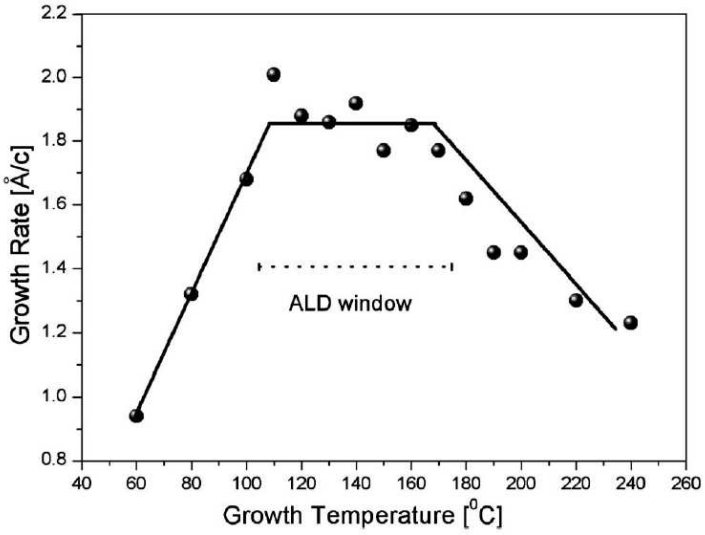

Figure 6.2: ALD growth window for ZnO growth using DEZn and H_2O as precursors.[12]

6.3.2 Substrates

In heteroepitaxy the simplest choice for the substrate is one with the same lattice structure and similar lattice parameters. Alternatively epitaxial crystal growth can occur if there exists a simple relationship between the structures of the substrate and crystal layer, such as with Al_2O_3 (100) and Si (100). In both cases a close match in the lattice parameters is required. Otherwise the strains induced by the lattice mismatch results in distortion of the film and formation of dislocations. If the mismatch is significant, epitaxial growth is not energetically favorable, causing a textured film or polycrystalline untextured film to be grown. As a general rule of thumb, epitaxy can be achieved if the lattice parameters of the two materials are within about 5% of each other. For good quality epitaxy the mismatch should be less than 1%. The larger the mismatch, the larger the strain in the film. As the film grows thicker, it will try to relieve the strain in the film, which can result in generation of dislocations or grain boundaries in the growing film.[91]

Sapphire (Al_2O_3) has been conventionally the most popular substrate for ZnO growth because of its low cost, availability as large-area wafers and its wide energy-band gap despite its poor structural and thermal match to ZnO.[2] The lattice mismatch is at minimum about 18 % [66], depending on the crystal orientation. Therefore more suitable substrates are also applied,

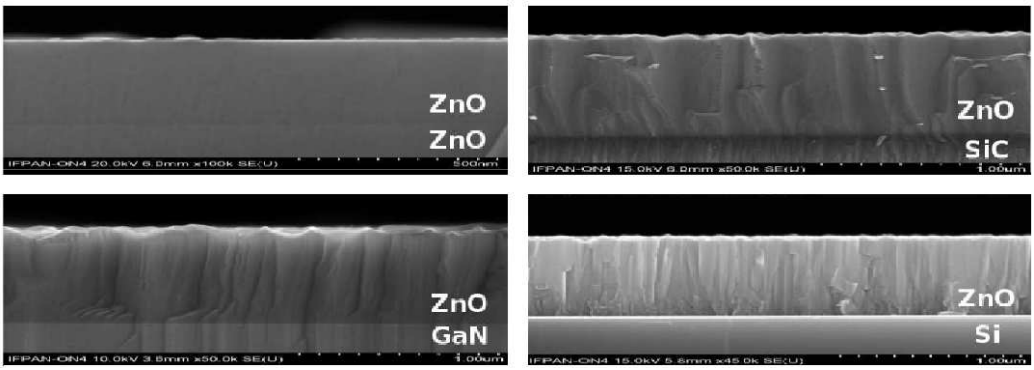

Figure 6.3: SEM images of ALD grown ZnO layers on ZnO bulk crystal, GaN, SiC and Si substrates. The best crystalline quality was obtained for ZnO and GaN substrates.[66]

such as YSZ (lattice mismatch about 10%) [14], silicon (lattice mismatch about 40 % [66]), SiC (lattice mismatch about 5 %) [66], GaN (mismatch is about 1.8 % [67]) and ZnO bulk crystal, having no lattice mismatch [66]. In Figure 6.3 there are cross-cut SEM images of ALD ZnO grown at 300°C on different substrates. The growth is visually columnar in all cases except the ZnO bulk crystal substrate, originating from the lattice mismatch and dislocations of the substrates. The best crystalline quality was obtained for ZnO and GaN substrates.[66]

As can be seen from the lattice mismatch values, in practice the substrate requirement of less than 1% mismatch is difficult to follow. The only substrate candidate with no lattice mismatch issues is ZnO bulk crystal, but the overall quality and availability have caused difficulties with its applications.[99] Due to the relatively small difference in the lattice constants of GaN and ZnO [100], GaN is considered currently the most suitable substrate material for epitaxial ZnO deposition.[10, 12, 14] In Figure 6.4 there is a transmission electron microscopy (TEM) image of the interface of epitaxial ZnO on GaN grown at 300°C, showing continuous crystal structure with no distinguishable interface layer.[101] The image confirms the suitability of GaN substrate for epitaxial ZnO growth.

6.3.3 Alternative growth methods

There are some alternative ways to grow epitaxial ZnO ALD films: using suitable buffer layer [96, 102–104], applying an electric field over the substrate

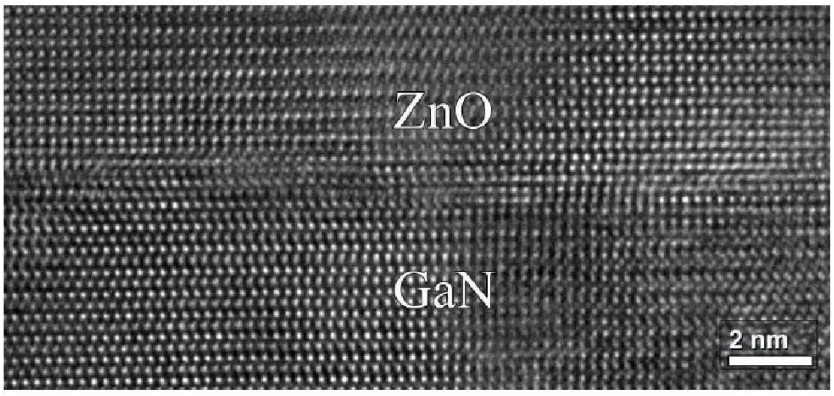

Figure 6.4: TEM image of the interface of epitaxial ZnO on GaN.[101]

[105] or a novel process called the interrupted flow method [106, 107].

In the case of applying buffer layer, the substrate can be also silicon or sapphire despite the poor lattice match. The buffer layer can be grown by ALD [96, 102, 104] or other growth method (such as CVD [103]). The function of the buffer layer is to form more lattice-matched basis for the epitaxial growth than the original substrate is.

When applying an electric field over the substrate, epitaxial ZnO film is reported to be achieved on sapphire substrate, when otherwise with the same growth parameters (but without the electric field) the resulting film is randomly oriented, polycrystalline film. This is explained by polarization of precursor molecules; it aligns them and that way direct the film growth on the substrate. The effect is seen already at growth temperature of 130°C, but the best result is at 600°C.[105]

In the flow-rate interruption (FRI) method the chamber is closed with an additional valve so that the precursor flow is not continuous, but the chamber stays in a steady condition during the precursor pulses. The main influence of this step is to enhance the precursor density in the reactor and to extend the duration of reaction between the reactant and the sample surface. This enables extremely low growth temperatures, when usually at very low temperatures the growth rate decreases and a conformal monolayer is not deposited because the thermal budget is insufficient. With FRI the optimal growth temperature range is between 60-200°C with sapphire substrate.[106, 107]

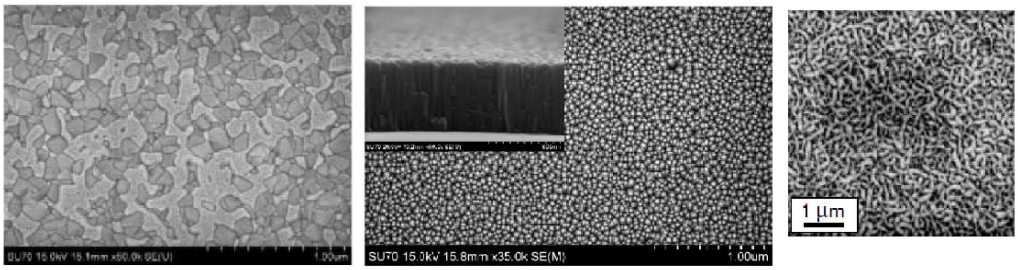

Figure 6.5: SEM images showing surface morphologies of ALD grown epitaxial ZnO from other reports with similar growth conditions (growth temperature of 300 °C): (a) [12] (b) [10] (c) [108].

6.4 Layer quality

The measurement results of the samples grown for this work are analyzed and compared to the other reports of ALD grown epitaxial ZnO on GaN in the next subsections. The results are also partly published in Journal of Crystal Growth [90].

6.4.1 Surface morphology

SEM images of the ZnO film surfaces are shown in Figure 6.1.[90] As can be seen from the images, the film structure changes with growth temperature. In the sample grown at 280 °C the surface structure seems to consist of partially merged grains with thick and clearly distinctive grain boundaries. Rough and granular surface is common for ALD grown epitaxial ZnO films, as can be seen in Figure 6.5 representing SEM images from other reports with similar growth conditions.[10, 12, 108] The surface of the sample grown at 290 °C consists of larger 3-dimensional flakes. However, when the growth temperature is increased, the flakes are merged together and the surface flattens. In the sample grown at 300 °C there are some additional step-like features and white artifacts, but ignoring them the surface is quite flat. The sample grown at 325 °C has a fully flat surface with no 3-dimensional structures. This is contradictory to previous reports of ALD grown ZnO films with similar growth parameters where flat surface was not achieved at 300 °C [10, 12, 108], represented in Figure 6.5. Surface flattening is most probably caused by increased re-evaporation and surface migration at higher growth temperature.[72, 109]

Even though the surface flattens with increasing growth temperature, pits with approximately 10 nm radius remain on the surface. The density of pits is approximately 10^{10} cm^{-2} in the sample grown at 325 °C (Fig. 6.1 (d)). The pits result most likely from coalescence boundaries of adjacent grains or from threading dislocation points of the GaN template surfaces. The threading dislocation density of the GaN templates was approximately 10^{9} cm^{-2}.

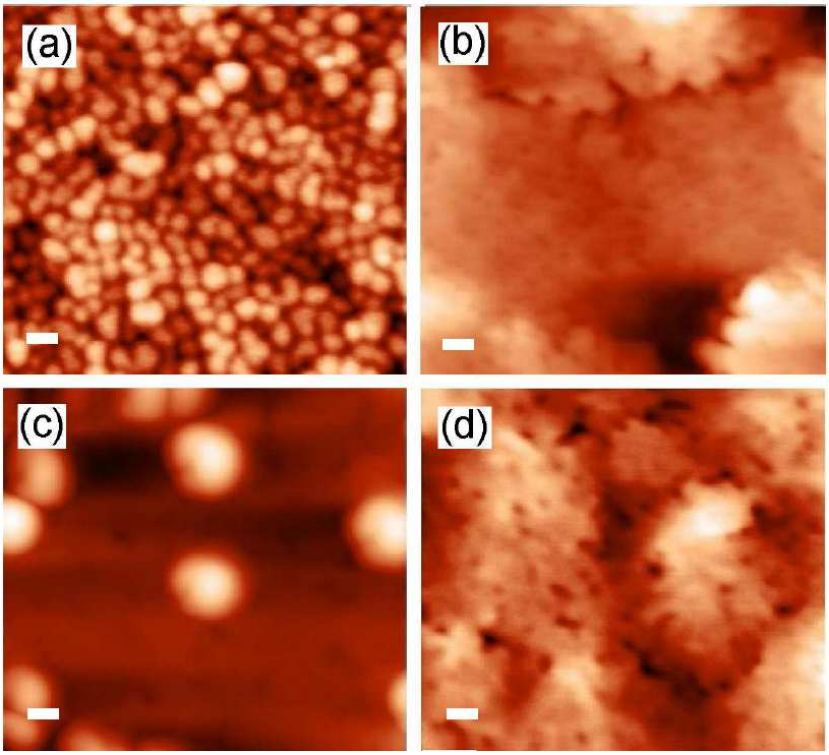

Figure 6.6: AFM images of the surfaces of the four samples. The scale bars correspond to 100 nm.

Figure 6.6 represents the AFM images of the four sample surfaces. As already seen in the SEM image (Figure 6.1), there are additional white artifacts on the surface of the sample grown in 300°C that are clearly disturbing the color scale of the AFM image. Otherwise the merging of the flakes and the surface flattening due to the increasing growth temperature can be clearly seen also in the AFM images.

Table 6.1: Surface roughness values [nm] of the four samples measured with AFM.

Growth temperature °C	Surface roughness (RMS) nm
280	1.56
290	1.921
300	1.597
325	0.606

In Table 6.1 there are listed the surface roughness values (RMS) for the four samples. The values are measured with AFM in areas where there are no white artifacts. Surface roughness decreases when the growth temperature increases, as expected based on the SEM images, and the roughness value of the last sample is extremely small, only 0.606 nm. The RMS value of the sample grown in 280°C seems to be abnormally small compared to the other samples. It is possible that the clearly multigrain surface structure on the sample grown in 280° C is on the average actually more flat than the sample grown in 290°C where there seems to be only few deeper grain boundaries in the SEM image. There are only two other reports of AFM results of ALD grown epitaxial ZnO on GaN, other one of them applying different precursors.[14, 110] The RMS value for the one with the same precursors (and growth temperature of 300°C) is 4.6 nm [14] and for the other applying different precursors ($ZnCl_2$ and O_2) and growth temperature of 480°C the RMS value is 0.45 nm [110]. However, the surface roughness values can be small even if the layer structure is polycrystalline.

6.4.2 Crystalline quality

The reciprocal space maps (RSMs) around the 002 reflection from samples grown at 280°C and 325°C are shown in Figures 6.7 (a) and (b), respectively. [90] For both samples, the GaN maximum is found at $H_\perp$ ∼0.3855 and the ZnO contribution at a smaller $H_\perp$ value. Both peaks are located at the same value (∼0) of the parallel component $H_\parallel$ of the reciprocal lattice vector H, indicating the ZnO layers have grown coherently on GaN and have (00j) planes parallel to each other. The small offset of $H_\parallel$ is due to inaccuracy in the calibration of the angle between the incident beam and the sample surface. The deviation of the zero position does however not influence other

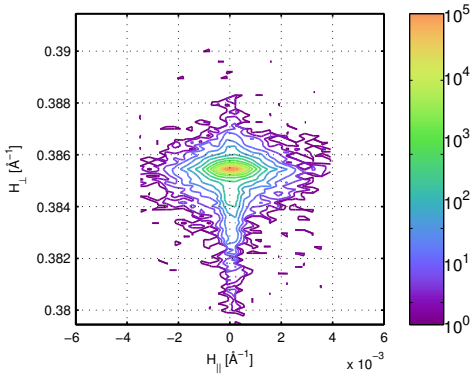

(a) Growth temperature 280 °C

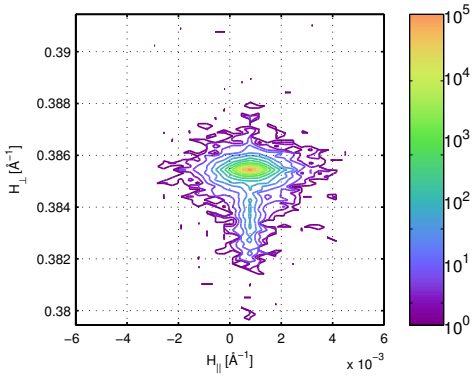

(b) Growth temperature 325 °C

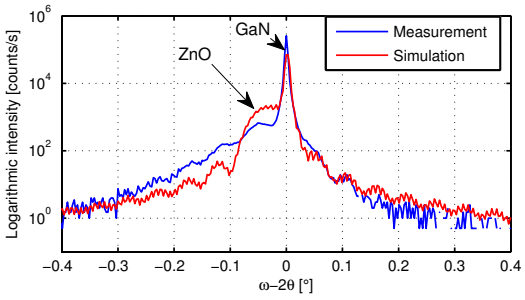

(c) Growth temperature 280 °C

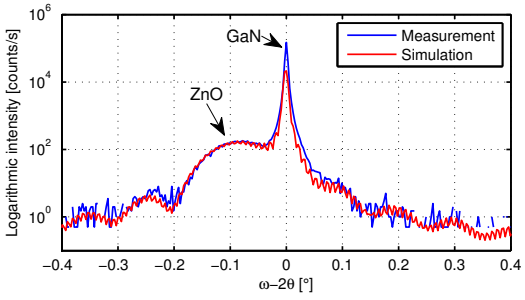

(d) Growth temperature 325 °C

Figure 6.7: Reciprocal space maps and XRD rocking curves for the samples grown at 280 °C and 325 °C.[90]

aspects of the RSMs. It is seen in figures 6.7 (a) and (b) that the diffraction image of the sample grown at 325°C is narrower in the $H_{\parallel}$ direction. This suggests that the sample grown at 325°C has less c-plane lattice tilt than the sample grown at 280°C and is therefore of better crystal quality [111, 112]. The more prominent lattice tilt in the sample grown at 280°C is most probably a result of the columnar ZnO structure, seen in Figure 6.1.

Figures 6.7 (c) and (d) show XRD scans and simulations around symmetric (002) planes of GaN and ZnO for the samples grown at 280°C and 325°C, respectively.[90] A ZnO peak is seen in both XRD ω-2θ scans on the low angle side of the high intensity GaN peak. Additionally, several thickness fringes are resolved in Figure 6.7 (c) and one clear fringe in Figure 6.7 (d). In absence of other broadening factors, the width of the XRD peak is dominated by layer thickness and increases with decreasing layer thickness[85]. Thicknesses of the ZnO layers were extracted from the simulation and are approximately 89 nm and 46 nm for samples grown at 280°C and 325°C, respectively. They correspond to growth rates of 0.89 Å and 0.46 Å per cycle. The difference in thicknesses may be explained by the morphological differences seen in SEM images 6.1 (a) and (d) and also by increased desorption and re-evaporation with increasing growth temperature. As illustrated in Figure 6.2, the ALD growth window for ZnO growth is about between 100-180°C [12], where the growth rate is 1.8-1.9 Å per cycle. Above the maximum temperature of the ALD growth window desorption and re-evaporation increase with increasing temperature and the growth rate decreases.[26, 72] At higher temperatures also the thermal decomposition of DEZn molecules causes the increase of residual impurities on the film surface. The density of surface OH groups acting as adsorption/reaction sites for metal precursors decreases, causing the decrease of the growth rate.[109]

As can be seen in Figures 6.7 (c) and (d), the fitting is significantly better for the sample grown at 325°C (Fig.6.7 (d)). The rather large discrepancy between the fitted and measured curves for the sample grown at 280°C (Fig. 6.7 (c)) can be attributed to the inhomogeneous granular structure of the ZnO layer grown at 280°C which cannot be fitted properly. As seen in the SEM images, the sample grown at 280°C (Fig.6.1 (a)) consists of partially merged grains with strong grain boundaries, whereas the surface of the sample grown at 325°C (Fig. 6.1 (d)) is completely 2-dimensional and smooth. This is also in accordance with the ZnO XRD peak positions in Figures 6.7 (c) and (d). The ZnO lattice constants were determined using their relative displacement from the GaN peaks calculated from the reciprocal space maps in Figures 6.7 (a) and (b). The ZnO lattice constants were found to be 5.204 Å and 5.218

Å for samples grown at 280°C and 325°C, respectively. The lattice constant 5.204 Å is very close to the reported bulk value of ZnO 5.204-5.207 Å [2] and indicates a relaxed growth, which is expected for a columnar structure. The larger lattice constant for the sample grown at 325°C indicates out of plane lattice expansion and in-plane lattice compression. Due to the lack of columnar structure and the presence of strain, the ZnO layer grown at 325°C is concluded to be epitaxially grown on the GaN template.

6.4.3 Optical properties

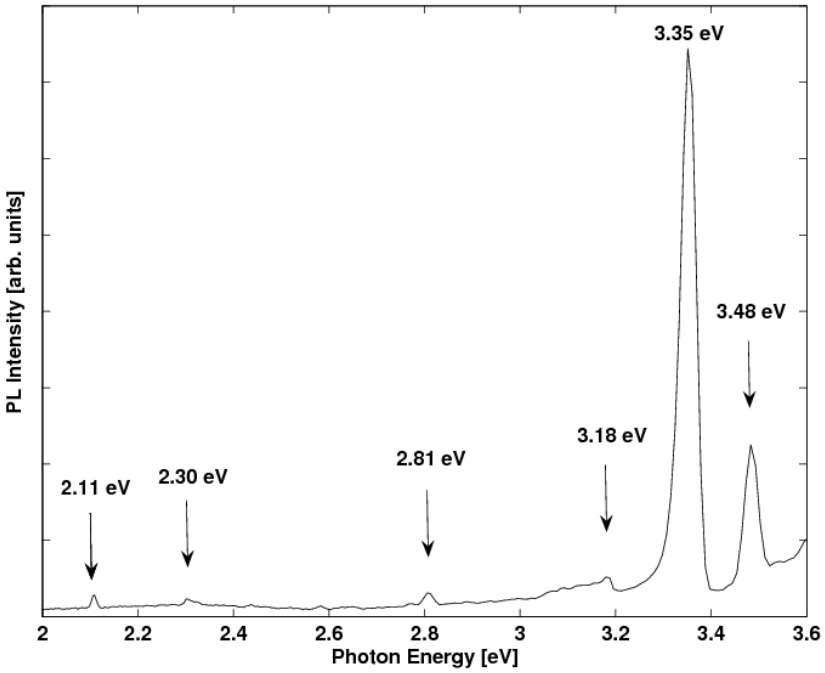

Figure 6.8: PL spectrum of ZnO sample with growth temperature of 325 °C, measured at 9 K.[90]

Fig. 6.8 shows the PL spectrum measured at 9 K for the sample grown at 325 °C.[90] The PL spectra of samples grown at lower temperatures were similar. There are two sharp peaks in every PL spectrum, at 3.48 eV (GaN template) and at 3.35 eV, that is the UV excitonic emission peak in ZnO originating from neutral donor-bound excitons (D^0X). At low temperatures the bound exciton emission dominates, which is known to be highly localized. Observation of excitonic emissions is commonly treated as an indication of good quality of the films.[16, 113] In addition to the GaN and ZnO (UV)

peaks, there are also four small peaks in the visible light region of the spectrum. The peak at 3.18 eV is either phonon replica of donor-bound exciton (DX-3LO) or donor-acceptor pair (DAP) transition. Other three peaks located at 2.11, 2.30 and 2.81 eV are in the low-energy range, where the green luminescence band is commonly observed. The detected peaks most probably originate from native point defects, such as oxygen and zinc vacancies.[2, 65]. The properties of ZnO PL spectrum are discussed in detail in Section 3.3.5.

Table 6.2: FWHM values for the ZnO excitonic peaks from reports of similar ALD growth conditions and from MBE and MOCVD reports.

Growth method	Reference	FWHM meV
ALD (this work)	[90]	7
ALD	[15]	16.1
ALD	[66]	4
ALD	[8]	6.1
ALD	[10]	13
MBE	[4]	5.7
MBE	[114]	5.5
MOCVD	[3]	3
MOCVD	[115]	8.3

No change was observed in the full width at half maximum (FWHM) values for the ZnO excitonic peaks of the four samples; they are all approximately 7 meV. The FWHM values are of the same magnitude as some of the previous reports of similar ALD growth conditions, as listed in Table 6.2.[8, 10, 15, 66] It is presumed that the layer quality does not substantially affect the excitonic emission in our samples, because the bound excitons are highly localized and the layer quality of the sample grown even at 280 °C appears to be good inside the grains. Reports of epitaxial ZnO growth by MBE [4, 114] and MOCVD [3, 115] show also FWHM values of the same magnitude (as listed in Table 6.2), although the growth temperatures are considerably higher (450-600 °C).

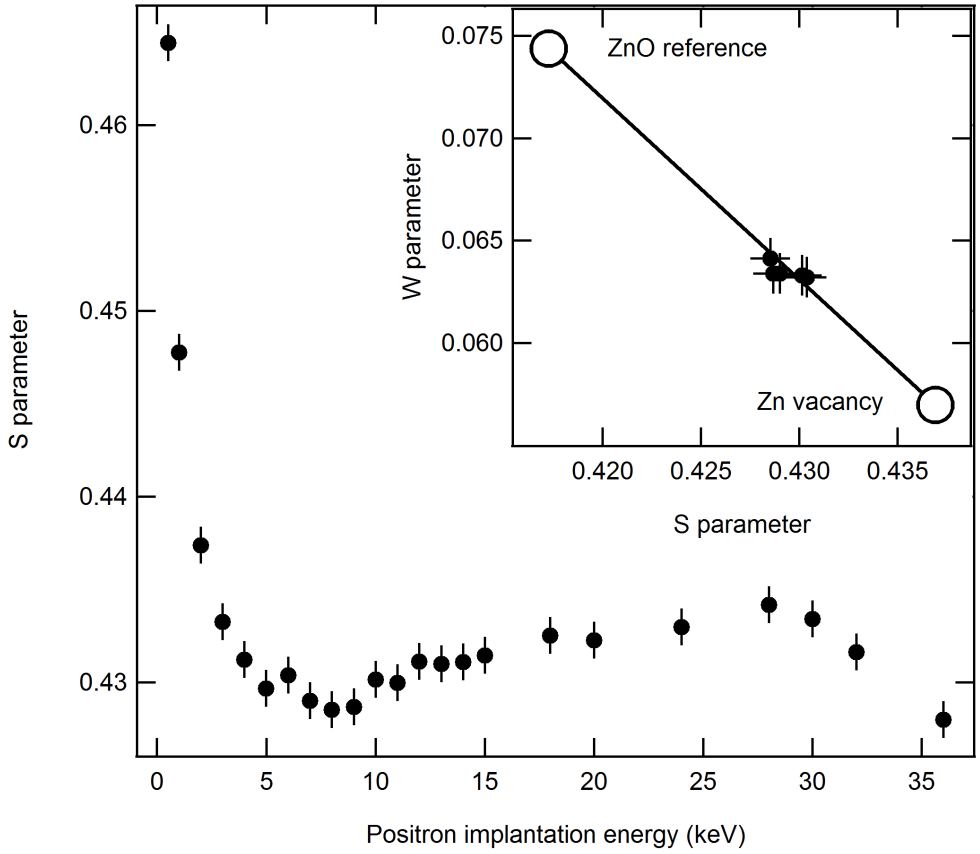

Figure 6.9: S parameter as a function of positron implantation energy (probing depth) in a ZnO sample. The ZnO layer is visible at positron energies 6 - 10 keV. At lower energies part of the positrons probe the surface of the sample. At energies 10 - 30 keV, positrons annihilate in the GaN template, and above 30 keV part of the positrons enter the sapphire substrate. The inset shows the (S, W) plot with the data from the ZnO layer, a ZnO reference and the point typical of single Zn vacancies [116].[90]

6.4.4 Zn vacancies

One ZnO sample (growth temperature 300 °C with 10 000 ALD cycles) was analyzed with positron annihilation spectroscopy (Fig. 6.9 [90]). The expected film thickness, 600 nm, corresponds well to the 10 keV positron implantation energy above which the GaN template becomes visible in the S parameter [117]. The results (inset of Fig. 6.9) show that Zn-vacancy related defects are present in the films with a concentration of roughly 3×10^{17}

cm^{-3}, similar to that typical of epitaxial films grown by MBE or MOCVD [116, 118]. There are no other reports of positron annihilation measurements of ALD grown ZnO. Interestingly, no clusters of vacancies were observed in the film, in spite of the rather high density of surface pits and the propensity of thin film ZnO containing vacancy clusters in concentrations significant enough to screen the Zn-vacancy related signal, regardless of the growth method [119].

6.4.5 Annealing

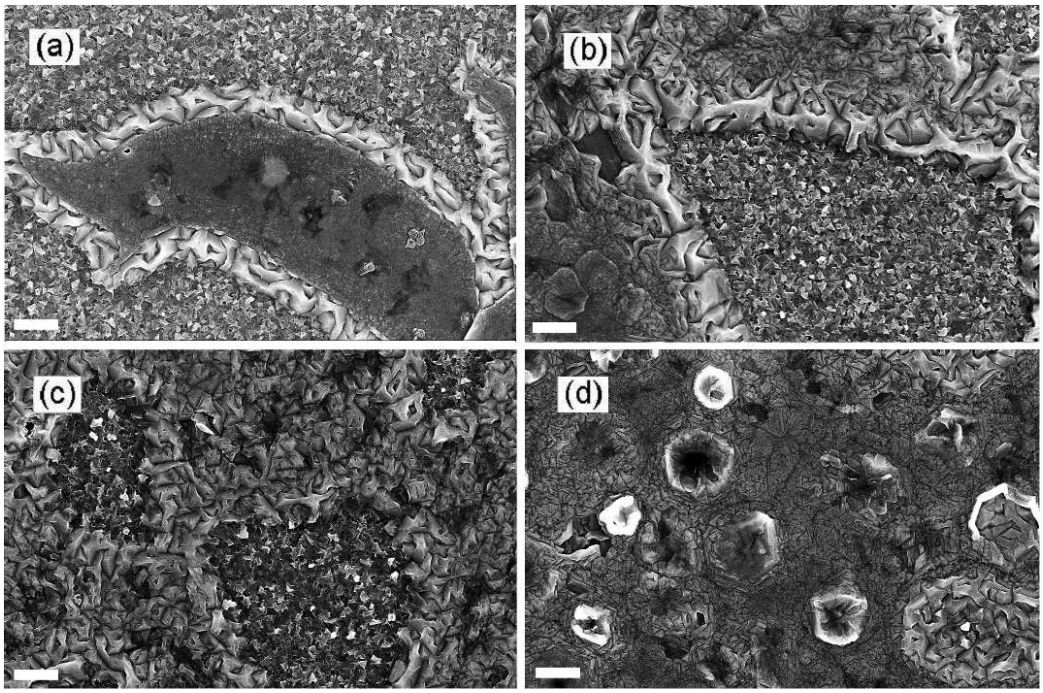

Figure 6.10: SEM images of the same samples after 1 hour annealing in 1000 °C oxygen environment. ZnO layer has peeled off and formed highly hexagonal substructures. The scale bars correspond to 1 μm.

The samples were finally annealed in 1000°C oxygen environment for 1 hour, and SEM images in Figure 6.10 reveal that the ZnO layer was damaged. In all the four samples the ZnO layer has peeled off, forming highly hexagonal substructures. This is unexpected result, because in two previous reports [16, 76] the same annealing procedure has resulted in distinct improvement of optical properties of the films. On the contrary, the previous reports conclude that annealing temperature of 1000°C is clearly more

effective than 800°C or lower temperatures, presenting also SEM images of enhanced crystallinity of the sample surface (Figure 6.11 [76]). There are no signs of layer damage in the SEM image. In both previous reports the ALD growth temperature was 170-400°C and the substrate sapphire, resulting in polycrystalline ZnO layer.[16, 76] However, these factors do not explain the major differences in the end results of the annealing experiments between the previous and this work.

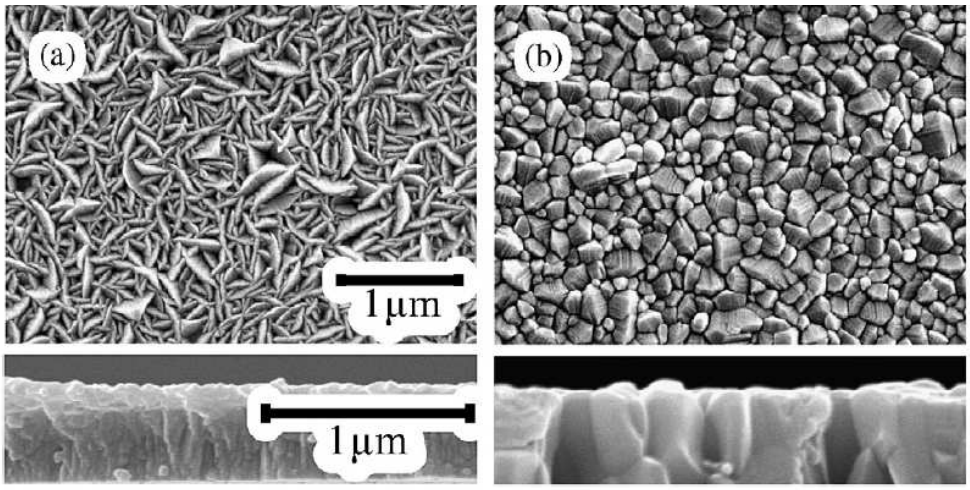

Figure 6.11: SEM images of a) ZnO sample grown at 170°C on sapphire substrate and b) the same sample after 1 hour annealing in 1000 °C oxygen environment. The annealing has clearly resulted in grain size growth.[76]

Chapter 7

Summary

This work represents the detailed fundamentals of ALD growth of epitaxial ZnO, familiarizing first separately with the basic characteristics of ZnO and ALD. Zinc oxide (ZnO) is a wide bandgap semiconductor with a variety of useful properties that have made it an object of increasing attention in numerous fields of research. The high transparency of ZnO to visible light combined with its tunable electrical conductivity enable its use in applications ranging from thin film transistors (TFTs) to the buffer layers of solar cells. The direct bandgap of ZnO around 3.4 eV at room temperature also enables many optoelectronic applications in the near-UV spectral range, including light-emitting diodes (LEDs) and photodetectors. Due to its piezoelectrical properties, ZnO is also used in micro-electromechanical applications.

Atomic layer deposition (ALD) enables conformal layer growth with precise thickness control. With ALD, other factors that precursors, substrate and growth temperature have little or no influence on the growing film. Epitaxial growth of ZnO can be achieved with ALD at relatively low temperature compared to other growth methods. There are also some novel, alternative growth methods for ALD that allow low-temperature high-quality epitaxial ZnO growth even on substrates with poor lattice match, such as sapphire and silicon. ALD grown epitaxial ZnO has some promising applications in semiconductor devices with 3D architecture and also with low-temperature limitations. Strong room-temperature luminescence and high transparency to visible light are properties that enables the epitaxial ZnO applications in optoelectronics and optics.

In this work we also report on the experimental results of the growth of epitaxial ZnO on GaN template by the ALD method. The threshold temperature for two dimensional growth is found to be approximately 290 °C

and the thin film quality further improves with elevated growth temperatures. Positron experiments also further confirm the high quality of the ZnO films: only defects related to single Zn vacancies (instead of clusters of vacancies) were detected. Contrary to previous reports, high-temperature annealing did not enhance the film properties but rather damaged the film. However, it can be concluded that ALD can be used to grown high quality ZnO films on GaN using diethylzinc and water vapour as precursors.

Bibliography

[1] C. Klingshirn: *ZnO: From basics towards applications*, Physica Status Solidi (b) 244 (2007) 3027.

[2] U. Özgür, Y. I. Alivov, C. Liu, A. Teke, M. A. Reshchikov, S. Doğan, V. Avrutin, S.-J. Cho and H. Morkoç: *A comprehensive review of ZnO materials and devices*, Journal of Applied Physics 98 (2005) 041301.

[3] S. Jung, W. Park, H. Cheong, G.-C. Yi, H. Jang, S. Hong and T. Joo: *Time-resolved and time-integrated photoluminescence in ZnO epilayers grown on Al_2O_3 (0001) by metalorganic vapor phase epitaxy*, Applied Physics Letters 80 (2002) 1924.

[4] P. Fons, K. Iwata, S. Niki, A. Yamada and K. Matsubara: *Growth of high-quality epitaxial ZnO films on α-Al_2O_3*, Journal of Crystal Growth 201/202 (1999) 627.

[5] J. Zhao, L. Hu, Z. Wang, Z. Wang, H. Zhang, Y. Zhao and X. Liang: *Epitaxial growth of ZnO thin films on Si substrates by PLD technique*, Journal of Crystal Growth 280 (2005) 455.

[6] A. Nahhas, H. Kim and J. Blachere: *Epitaxial growth of ZnO films on Si substrates using an epitaxial GaN buffer*, Applied Physics Letters 78 (2001) 1511.

[7] S. George: *Atomic Layer Deposition: An Overview*, Chemical Reviews 110 (2010) 111.

[8] L. Wachnicki, M. Lukasiewicz, B. Witkowski, T. Krajewski, G. Łuka, K. Kopalko, R. Minikayev, E. Przeździecka, J. Domagala, M. Godlewski and E. Guziewicz: *Comparison of dimethylzinc and diethylzinc as precursors for monocrystalline zinc oxide grown by atomic layer deposition method*, Physica Status Solidi B 247 (2010) 1699.

[9] R. Triboulet and J. Perrière: *Epitaxial growth of ZnO films*, Progress in Crystal Growth and Characterization of Materials 47 (2003) 65.

[10] L. Wachnicki, T. Krajewski, G. Łuka, B. Witkowski, B. Kowalski, K. Kopalko, J. Domagala, M. Guziewicz, M. Godlewski and E. Guziewicz: *Monocrystalline zinc oxide films grown by atomic layer deposition*, Thin Solid Films 518 (2010) 4556.

[11] T. Tynell and M. Karppinen: *Atomic layer deposition of ZnO: a review*, Semiconductor Science and Technology 29 (2014) 043001.

[12] E. Guziewicz, M. Godlewski, T. Krajewski, L. Wachnicki, G. Łuka, J. Dogamala, W. Paszkowicz, B. Kowalski, B. Witkowski, A. Dużyńska and A. Suchock: *Zinc oxide grown by atomic layer deposition - a material for novel 3D electronics*, Physica Status Solidi (b) 247 (2010) 1611.

[13] V. Miikkulainen, M. Leskelä, M. Ritala and R. Puurunen: *Crystallinity of inorganic films grown by atomic layer deposition: Overview and general trends*, Journal of Applied Physics 113 (2013) 021301.

[14] C.-W. Lin, D.-J. Ke, Y.-C. Chao, L. Chang, M.-H. Liang and Y.-T. Ho: *Atomic layer deposition of epitaxial ZnO on GaN and YSZ*, Journal of Crystal Growth 298 (2007) 472.

[15] K. Saito, K. Nagayama, Y. Hosokai, K. Ishida and K. Takahashi: *Effects of GaN template on atomic-layer-epitaxy growth of ZnO*, Physica Status Solidi (c) 1 (2004) 969.

[16] J. Lim, K. Shin, H. Kim and C. Lee: *Photoluminescence Studies of ZnO thin films grown by atomic layer epitaxy*, Journal of Luminescence 109 (2004) 181.

[17] A. Wójcik, K. Kopalko, M. Godlewski, E. Lusakowska, E. Guziewicz, R. Minikayev, W. Paszkowicz, K. Swiatek, M. Klepka, R. Jakiela, M. Kiecana, M. Sawicki, K. Dybko and M. Phillips: *Thin films of ZnO and ZnMnO by atomic layer epitaxy*, Optica Aplicata 35 (2005) 413.

[18] C. Kim, C. Shin, J. Lee, J. Heo, T. Lee, J. Park, H. Ryu, C. Son and J. Chang: *Influence of annealing duration on optical property and surface morphology of ZnO thin film grown by atomic layer deposition*, Current Applied Physics 10 (2010) S294.

[19] C.-Y. Yen, S.-R. Jian, G.-J. Chen, C.-M. Lin, H.-Y. Lee, W.-C. Ke, Y.-Y. Liao, P.-F. Yang, C.-T. Wang, Y.-S. Lai, J. S.-C. Jang and J.-Y. Juang: *Influence of annealing temperature on the structural, optical and mechanical properties of ALD-derived ZnO thin films*, Applied Surface Science 257 (2011) 7900.

[20] J. Lim, H. K. K. Shin and C. Lee: *Effect of annealing on the photoluminescence characteristics of ZnO thin films grown on the sapphire substrate by atomic layer epitaxy*, Materials Science and Engineering B 107 (2004) 301.

[21] S.-Y. Pung, K.-L. Choy, X. Hou and C. Shan: *Preferential growth of ZnO thin films by the atomic layer deposition technique*, Nanotechnology 19 (2008) 435609.

[22] R. Puurunen: *Surface chemistry of atomic layer deposition: A case study for the trimethylaluminum/water process*, Journal of Applied Physics 97 (2005) 121301.

[23] L. Niinistö, J. Päiväsaari, J. Niinistö, M. Putkonen and M. Nieminen: *Advanced electronic and optoelectronic materials by Atomic Layer Deposition: An overview with special emphasis on recent progress in processing of high-κ dielectrics and other oxide materials*, Physica Status Solidi (a) 201 (2004) 1443.

[24] Stanford Nanofabrication Facility: *Labmembers Wiki: Equipment introduction to ALD device Savannah* (2014), `https://snf.stanford.edu/SNF/equipment/chemical-vapor-deposition/ald/savannah-images/ald1.jpg/`. Accessed 10.5.2014.

[25] M. Leskelä and M. Ritala: *Atomic layer deposition (ALD): from precursors to thin film structures*, Thin Solid Films 409 (2002) 138.

[26] Z. Baji, Z. Lábadi, Z. Horváth, G. Molnár, J. Volk, I. Bársony and P. Barna: *Nucleation and Growth Modes of ALD ZnO*, Crystal Growth & Design 12 (2012) 5615.

[27] T. Suntola and J. Antson: *U.S. Patent No. 4,058,430* (15.11.1977), `https://www.google.com/patents/US4058430` Accessed 11.5.2014.

[28] M. Godlewski: *Editorial: Atomic layer deposition*, Semiconductor Science and Technology 27 (2012) 070301.

[29] M. Knez, K. Nielsch and L. Niinistö: *Synthesis and Surface Engineering of Complex Nanostructures by Atomic Layer Deposition*, Advanced Materials 19 (2007) 3425.

[30] J. Swart (ed.): *Solid State Circuits Technologies*, InTech, 2010.

[31] J. Kittl, K. Opsomer, M. Popovici, N. Menou, B. Kaczer, X. Wang, C. Adelmann, M. Pawlak, K. Tomida, A. Rothschild, B. Govoreanu, R. Degraeve, M. Schaekers, M. Zahid, A. Delabie, J. Meersschaut, W. Polspoel, S. Clima, G. Pourtois, W. Knaepen, C. Detavernier, V. Afanas'ev, T. Blomberg, D. Pierreux, J. Swerts, P. Fischer, J. Maes, D. Manger, W. Vandervorst, T. Conrad, A. Franquet, P. Favia, H. Bender, B. Brijs, S. van Elshocht, M. Jurczak, J. van Houdt and D. Wouters: *High-κ Dielectrics and Metal Gates for Future Generation Memory Devices*, ECS Transactions 19 (2009) 29.

[32] S. Chambers: *Ferromagnetism in doped thin-film oxide and nitride semiconductors and dielectrics*, Surface Science Reports 61 (2006) 345.

[33] M. Sellers and E. Seebauer: *Structural and magnetic properties of Mn-doped anatase TiO_2 films synthesized by atomic layer deposition*, Applied Physics A 104 (2011) 583.

[34] S. Bystrova: *Diffusion barriers for Cu metallisation in Si integrated circuits*, Ph.D. thesis, Semiconductor Components (SC) group, MESA+ research institute/University of Twente, The Netherlands (2004), `http://doc.utwente.nl/48234/1/thesis_Bystrova.pdf/`.

[35] I. Dirnstorfer: *Passivation Layers for Solar Cells* (2014), `http://www.namlab.com/pages/en_research_applications_energyharvesting.htm/`. Accessed 22.5.2014.

[36] Y. Geng, L. Guo, S.-S. Xu, Q.-Q. Sun, S.-J. Ding, H.-L. Lu and D. W. Zhang: *Influence of Al Doping on the Properties of ZnO Thin Films Grown by Atomic Layer Deposition*, The Journal of Physical Chemistry C 115 (2011) 12317.

[37] Beneq: *nSILVER Anti-tarnish Coating* (2010), `http://www.beneq.com/nsilver-anti-tarnish-coating.html/`. Accessed 13.5.2014.

[38] G. Parsons, J. Elam, S. George, S. Haukka, H. Jeon, W. Kessels, M. Leskelä, P. Poodt, M. Ritala and S. M. Rossnagel: *History of atomic layer deposition and its relationship with the American Vacuum Society*, Journal of Vacuum Science & Technology A 31 (2013) 050818.

[39] C. Klingshirn: *ZnO: Material, Physics and Applications*, ChemPhysChem 8 (2007) 782.

[40] E. Wiberg and A. Holleman: *Inorganic Chemistry*, Elsevier, 2001.

[41] N. Greenwood and A. Earnshaw: *Chemistry of the Elements*, Oxford: Butterworth-Heinemann, 1997.

[42] C. Klingshirn, B. Meyer, A. Waag, A. Hoffmann and J. Geurts: *Zinc Oxide: From Fundamental Properties Towards Novel Applications*, Springer, 2010.

[43] H. Morkoç and U. Özgür: *Zinc Oxide: Fundamentals, Materials and Device Technology*, Wiley, 2009.

[44] T. Kogure and Y. Bando: *Formation of ZnO nanocrystallites on ZnS surfaces by electron beam irradiation*, Journal of Electron Microscopy 47 (1998) 135.

[45] A. Ashrafi, A. Ueta, A. Avramescu, H. Kumano, I. Suemune, Y.-W. Ok and T.-Y. Seong: *Growth and characterization of hypothetical zinc-blende ZnO films on GaAs(001) substrates with ZnS buffer layers*, Applied Physics Letters 76 (2000) 550.

[46] J. Jaffe, J. Snyder, Z. Lin and A. Hess: *LDA and GGA calculations for high-pressure phase transitions in ZnO and MgO*, Physical Review B 62 (2000) 1660.

[47] U. Rossler (ed.): *Landolt-Börstein, New Series, Group III, Vol. 17B*, Springer, 1999.

[48] J. R. Hook and H. E. Hall: *Solid State Physics, Second Edition*, Wiley, 2003.

[49] C. Rogers: *Solutions for homework in Introduction to Solid State Physics Course* (2003), `http://www.colorado.edu/physics/phys7440/phys7440_sp03/HOMEWORK/Homework/S8.htm/`. Accessed 2.2.2014.

[50] G. Sun: *The Intersubband Approach to Si-based Lasers, Chapter 13* (2010), `http://www.intechopen.com/books/advances-in-lasers-and-electro-optics/the-intersubband-approach-to-si-based-lasers/`. Accessed 25.12.2013.

[51] B. Streetman and S. Banerjee: *Solid State Electronic Devices*, 6th edition, Pearson Prentice Hall, 2006.

[52] P. Bhattacharya: *Semiconductor Optoelectronic Devices, Second Edition*, Prentice-Hall of India, 2007.

[53] C. Klingshirn: *Semiconductor Optics, Fourth Edition*, Springer, 2012.

[54] M. Glazer and G. Burns: *Space Groups for Solid State Scientists*, Academic Press, 2013.

[55] M. Wagner: *Optical Spectroscopy of Defects and Impurities in ZnO*, Ph.D. thesis, Institute of Solid State Physics, Faculty II: Mathematics and Science, Technical University Berlin, Berlin, Germany (2005), `http://www.physik.tu-berlin.de/~mwagner/thesis/wagner_diplom.pdf/`.

[56] Q. Xu, X.-W. Zhang, W.-J. Fan, S.-S. Li and J.-B. Xia: *Silicon photonics: Nanocavity brightens silicon*, Computational Materials Science 44 (2008) 72.

[57] C. Jagadish and S. Pearton: *Zinc Oxide Bulk, Thin Films and Nanostructures. Processing, Properties, and Applications*, Elsevier, 2006.

[58] J. Jaffe, R. Pandey and A. Kunz: *Electronic structure of the rocksalt-structure semiconductors ZnO and CdO*, Physical Review B 43 (1991) 14030.

[59] D. Holt and B. Yacobi: *Extended Defects in Semiconductors: Electronic Properties, Device Effects and Structures*, Cambridge University Press, 2007.

[60] Wikimedia Commons: *Point defects in crystal structures: Interstitial and substitutional atom, Vacancy, Frenkel defect* (2011), `http://commons.wikimedia.org/wiki/File:Point_defects_in_crystal_structures.svg/`. Accessed 22.2.2014.

[61] NDT Resource Center, NDT Course Material: *Materials and Processes: Point defects* (2008), `http://www.ndt-ed.org/EducationResources/CommunityCollege/Materials/Structure/point_defects.htm/`. Accessed 23.2.2014.

[62] M. McCluskey and S. Jokela: *Defects in ZnO*, Journal of Applied Physics 106 (2009) 071101.

[63] A. Janotti and C. V. de Walle: *Native point defects in ZnO*, Physical Rewiev B 76 (2007) 165202.

[64] B. van Zeghbroeck: *Principles of Semiconductor Devices, Chapter 2: Semiconductor Fundamentals* (2011), `http://ecee.colorado.edu/~bart/book/book/chapter2/ch2_6.htm#fig2_6_6/`. Accessed 18.2.2014.

[65] M. Wagner: *Fundamental properties of excitons and phonons in ZnO: A spectroscopic study of the dynamics, polarity, and effects of external fields*, Ph.D. thesis, Institute of Solid State Physics, Faculty II: Mathematics and Science, Technical University Berlin, Berlin, Germany (2010), `http://opus4.kobv.de/opus4-tuberlin/files/2727/wagner_markus.pdf/`.

[66] L. Wachnicki, A. Dużyńska, J. Domagala, B. Witkowski, T. Krajewski, E. Przeździecka, M. Guziewicz, A. Wierzbicka, K. Kopalko, S. Figge, D. Hommel, M. Godlewski and E. Guziewicz: *Epitaxial ZnO Films Grown at Low Temperature for Novel Electronic Application*, Acta Physica Polonica A 120 (2011) A.

[67] B. Ataev, W. Lundin, V. Mamedov, A. Bagamadova and E. Zavarin: *Low-pressure chemical vapour deposition growth of high-quality ZnO films on epi-GaN/α-Al_2O_3*, Journal of Physics: Condensed Matter 13 (2001) L211.

[68] U. Özgür, D. Hofstetter and H. Morkoç: *ZnO Devices and Applications: A Review of Current Status and Future Prospects*, Proceedings of the IEEE 98 (2010) 1255.

[69] I. Akasaki, H. Amano, Y. Koide, K. Hiramatsu and N. Sawaki: *Effects of ain buffer layer on crystallographic structure and on electrical and optical properties of GaN and $Ga_{1-x}Al_xN$ ($0 < x \leq 0.4$) films grown on sapphire substrate by MOVPE*, Journal of Crystal Growth 98 (1989) 209.

[70] T. Krajewski, E. Guziewicz, M. Godlewski, L. Wachnicki, I. A. Kowalik, A. Wójcik-Glodowska, M. Lukasiewicz, K. Kopalko, V. Osinniy and M. Guziewicz: *The influence of growth temperature and precursors' doses on electrical parameters of ZnO thin films grown by atomic layer deposition technique*, Microelectronics Journal 40 (2009) 1293.

[71] C. Thiandoume, V. Sallet, R. Triboulet and O. Gorochov: *Decomposition kinetics of tertiarybutanol and diethylzinc used as precursor*

sources for the growth of ZnO, Journal of Crystal Growth 311 (2009) 1411.

[72] S. Franssila: *Introduction to Microfabrication*, Wiley, 2007.

[73] H.-C. Chen, M.-J. Chen, M.-K. Wu, Y.-C. Cheng and F.-Y. Tsai: *Low-Threshold Stimulated Emission in ZnO Thin Films Grown by Atomic Layer Deposition*, IEEE Journal of Selected Topics in Quantum Electronics 14 (2008) 1053.

[74] H. Chen, M. Chen, T. Liu, J. Yang and M. Shiojiri: *Structure and stimulated emission of a high-quality zinc oxide epilayer grown by atomic layer deposition on the sapphire substrate*, Thin Solid Films 519 (2010) 536.

[75] H.-C. Chen, M.-J. Chen, M.-K. Wu, W.-C. Li, H.-L. Tsai, J.-R. Yang, H. Kuan and M. Shiojiri: *UV Electroluminescence and Structure of n-ZnO/p-GaN Heterojunction LEDs Grown by Atomic Layer Deposition*, IEEE Journal of Quantum Electronics 46 (2010) 265.

[76] J. Lim and C. Lee: *Effects of substrate temperature on the microstructure and photoluminescence properties of ZnO thin films prepared by atomic layer deposition*, Thin Solid Films 515 (2007) 3335.

[77] S. Yang, B. Lin, C. Kuo, H. Hsu, W.-R. Liu, M. Eriksson, P.-O. Holtz, C.-S. Chang, C.-H. Hsu and W. Hsieh: *Improvement of Crystalline and Photoluminescence of Atomic Layer Deposited m-Plane ZnO Epitaxial Films by Annealing Treatment*, Crystal Growth & Design 12 (2012) 4745.

[78] S. Yang, B. Lin, W.-R. Liu, J.-H. Lin, C.-S. Chang, C.-H. Hsu and W. F. Hsieh: *Structural Characteristics and Annealing Effect of ZnO Epitaxial Films Grown by Atomic Layer Deposition*, Crystal Growth & Design 9 (2009) 5184.

[79] S. Swapp: *Scanning Electron Microscopy (SEM)* (2013), `http://serc.carleton.edu/research_education/geochemsheets/techniques/SEM.html/`. Accessed 3.6.2014.

[80] H. Nykänen: *Low energy electron beam irradiation of gallium nitride*, Ph.D. thesis, Aalto University, Department of Micro- and Nanosciences, Finland (2013), `http://urn.fi/URN:ISBN:978-952-60-5445-2/`.

[81] J. W.D. Callister: *Materials Science and Engineering, An Introduction*, Wiley, 2003.

[82] K. Aggeliki: *Atomic Force Microscopy - AFM (Contact, Non-contact, and Semi-contact Modes)* (2011), `http://www.brighthubengineering.com/manufacturing-technology/95102-atomic-force-microscopy-afm-contact-non-contact-and-semi-contact-modes/`. Accessed 1.6.2014.

[83] T. Boyd and A.R. Barron: *An Introduction to Single-Crystal X-Ray Crystallography* (2013), `http://cnx.org/content/m46149/latest/?collection=col10699/latest/`. Accessed 2.6.2014.

[84] Evans Analytical Group: *X-ray Diffraction (XRD) Analysis* (2014), `http://www.eag.com/mc/x-ray-diffraction.html/`. Accessed 2.6.2014.

[85] P. F. Fewster: *X-ray Scattering from Semiconductors, 2nd edition*, Imperial College Press, London, 2003.

[86] University of Reading: *The atomic basis of matter. X-ray scattering and Bragg's law* (1996), `http://www.met.reading.ac.uk/pplato2/h-flap/phys7_1f_2.png/`. Accessed 4.6.2014.

[87] K. Shinde, S. Dhoble, H. Swart and K. Park: *Phosphate Phosphors for Solid-State Lighting*, Springer, 2012.

[88] R. Paschotta: *Field Guide to Lasers*, SPIE Press, 2008.

[89] P. Schultz and K. Lynn: *Interaction of positron beams with surfaces, thin films, and interfaces*, Review of Modern Physics 60 (1988) 701.

[90] S. Särkijärvi, S. Sintonen, F. Tuomisto, M. Bosund, S. Suihkonen and H. Lipsanen: *Effect of growth temperature on the epitaxial growth of ZnO on GaN by ALD*, Journal of Crystal Growth 398 (2014) 18.

[91] A. Barron and C. Smith: *Crystal Structure* (2013), `http://cnx.org/content/m16927/latest/?collection=col10699/latest/`. Accessed 6.6.2014.

[92] H. Kumagai, Y. Tanaka, M. Murata, Y. Masuda and T. Shinagawa: *Novel TiO_2/ZnO multilayer mirrors at 'water-window' wavelengths fabricated by atomic layer epitaxy*, Journal of Physics: Condensed Matter 22 (2010) 474008.

[93] K. Kopalko, A. Wójcik, M. Godlewski, E. Lusakowska, W. Paszkowicz, J. Domagala, M. Godlewski, A. Szczerbakow, K. Swiatek and K. Dybko: *Growth by atomic layer epitaxy and characterization of thin films of ZnO*, Physica Status Solidi C 2 (2005) 1125.

[94] A. Wójcik, K. Kopalko, M. Godlewski, E. Lusakowska, W. Paszkowicz, K. Dybko, J. Domagala, A. Szczerbakow and E. Kaminska: *Monocrystalline and Polycrystalline ZnO and ZnMnO films Grown by Atomic Layer Epitaxy - Growth and Characterization*, Acta Physica Polonica A 105 (2004) 667.

[95] H. Yuan, B. Luo, S. A. Campbell and W. Gladfelter: *Atomic Layer Deposition of p-Type Phosphorus-Doped Zinc Oxide Films Using Diethylzinc, Ozone and Trimethylphosphite*, Electrochemical and Solid-State Letters 14 (2011) H181.

[96] P.-Y. Lin, J.-R. Gong, P.-C. Li, T.-Y. Lin, D.-Y. Lyu, D.-Y. Lin, H.-J. Lin, T.-C. Li, K.-J. Chang and W.-J. Lin: *Optical and structural characteristics of ZnO films grown on (0 0 01) sapphire substrates by ALD using DEZn and N_2O*, Journal of Crystal Growth 310 (2008) 3024.

[97] K. Kaiya, N. Yoshii, K. Omichi, N. Takahashi, T. Nakamura, S. Okamoto and H. Yamamoto: *Atmospheric Pressure Atomic Layer Epitaxy of ZnO Using a Chloride Source*, Chemistry of Materials 13 (2001) 1952.

[98] S. Kim, C. Hwang, S.-H. Park and S. Yun: *Comparison between ZnO films grown by atomic layer deposition using H_2O or O_3 as oxidant*, Thin Solid Films 478 (2005) 103.

[99] R. Triboulet: *Growth of ZnO bulk crystals: A review*, Progress in Crystal Growth and Characterization of Materials 60 (2014) 1.

[100] V. Karpina, V. Lazorenko, C. Lashkarev, V. Dobrowolski, L. Kopylova, V. Baturin, S. Pustovoytov, A. Karpenko, S. Eremin, P. Lytvyn, V. Ovsyannikov and E. Mazurenko: *Zinc oxide - analogue of GaN with new perspective possibilities*, Crystal Research and Technology 39 (2004) 980.

[101] B. Pécz, Z. Baji, Z. Lábadi and A. Kovács: *ZnO layers deposited by Atomic Layer Deposition*, Journal of Physics: Conference Series 471 (2013) 012015.

[102] S. Lee, Y. H. Im, S. H. Kim and Y. B. Hahn: *Structural and optical properties of high quality ZnO films on Si grown by atomic layer deposition at low temperatures*, Superlattices and Microstructures 39 (2006) 24.

[103] C. Kim, J. Lee, C. Shin, J. Leem, H. Ryu, J. Chang, H. Lee, C. Son, W. Lee, W. Jung, S. Tan, J. Zhao and X. Sun: *Effects of annealing temperature of buffer layer on structural and optical properties of ZnO thin film grown by atomic layer deposition*, Solid State Communications 148 (2008) 395.

[104] Z. Baji, Z. Lábadi, G. Molnár, B. Pécz, K. Vad, Z. Horváth, P. Szabó, T. Nagata and J. Volk: *Highly conductive epitaxial ZnO layers deposited by atomic layer deposition*, Thin Solid Films 562 (2014) 485.

[105] C. Liu, M. Yan, X. Liu, E. Seelig and R. Chang: *Effect of electric field upon the ZnO growth on sapphire (0 0 0 1) by atomic layer epitaxy method*, Chemical Physics Letters 355 (2002) 43.

[106] C.-S. Ku, J.-M. Huang, C.-M. Lin and H.-Y. Lee: *Fabrication of epitaxial ZnO films by atomic-layer deposition with interrupted flow*, Thin Solid Films 518 (2009) 1373.

[107] J.-M. Huang, C.-S. Ku, H.-Y. Lee, C.-M. Lin and S.-Y. Chen: *Growth of high-quality epitaxial ZnO films on (10-10) sapphire by atomic layer deposition with flow-rate interruption method*, Surface & Coatings Technology 231 (2013) 323.

[108] B. Witkowski, L. Wachnicki, P. Nowakowski, A. Suchocki and M. Godlewski: *Temperature-dependence of cathodoluminescence of zinc oxide monolayers obtained by atomic layer deposition*, Optica Applicata 43 (2013) 187.

[109] H. Makino, A. Miyake, T. Yamada, N. Yamamoto and T. Yamamoto: *Influence of substrate temperature and Zn-precursors on atomic layer deposition of polycrystalline ZnO films on glass*, Thin Solid Films 517 (2009) 3138.

[110] K. Kopalko, M. Godlewski, J. Domagala, E. Lusakowska, R. Minikayev, W. Paszkowicz and A. Szczerbakow: *Monocrystalline ZnO Films on GaN/Al_2O_3 by Atomic Layer Epitaxy in Gas Flow*, Chemistry of Materials 16 (2004) 1447.

[111] M. Moram and M. Vickers: *X-ray diffraction of III-nitrides*, Reports on Progress in Physics 72 (2009) 036502.

[112] A. Dadgar, N. Oleynik, D. Forster, S. Deiter, H. Witek, J. Bläsing, F. Bertram, A. Krtschil, A. Diez, J. Christen and A. Krost: *A two-step metal organic vapor phase epitaxy growth method for high-quality ZnO on GaN/Al_2O_3 (0 0 0 1)*, Journal of Crystal Growth 267.

[113] B. Meyer, H. Alves, D. Hofmann, W. Kriegseis, D. Forster, F. Bertram, J. Christen, A. Hoffmann, M. Straßburg, M. Dworzak, U. Haboeck and A. Rodina: *Bound exciton and donor-acceptor pair recombinations in ZnO*, Physica Status Solidi (b) 241 (2004) 231.

[114] Y. Chen, D. Bagnall, Z. Zhu, T. Sekiuchi, K.-T. Park, K. Hiraga, T. Yao, S. Koyama, M. Shen and T. Goto: *Growth of ZnO single crystal thin films on c-plane (0 0 0 1) sapphire by plasma enhanced molecular beam epitaxy*, Journal of Crystal Growth 181 (1997) 165.

[115] A. Ashrafi, N. Binh, B. Zhang and Y. Segawa: *Temperature-dependent photoluminescence of ZnO layers grown on 6H-SiC substrates*, Journal of Applied Physics 95 (2004) 7738.

[116] A. Zubiaga, F. Tuomisto, V. Coleman, H. Tan, C. Jagadish, K. Koike, S. Sasa, M. Inoue and M. Yano: *Mechanisms of electrical isolation in O^+-irradiated ZnO*, Physical Review B 78 (2008) 035125.

[117] A. Zubiaga, J. García, F. Plazaola, F. Tuomisto, J. Z. niga Pérez and V. M. noz Sanjosé: *Positron annihilation spectroscopy for the determination of thickness and defect profile in thin semiconductor layers*, Physical Review B 75 (2007) 205305.

[118] A. Zubiaga, F. Tuomisto, F. Plazaola, K. Saarinen, J. Garcia, J. Rommeluere, J. Z. niga Pérez and V. M. noz Sanjosé: *Zinc vacancies in the heteroepitaxy of ZnO on sapphire: Influence of the substrate orientation and layer thickness*, Applied Physics Letters 86 (2005) 042103.

[119] V. Venkatachalapathy, A. Galeckas, A. Zubiaga, F. Tuomisto and A. Y. Kuznetsov: *Changing vacancy balance in ZnO by tuning synthesis between zinc/oxygen lean conditions*, Journal of Applied Physics 108 (2010) 046101.